

FINAL REPORT – YEAR 3

Texas Water Development Board contract 2002-483-440

QUANTIFYING SEDIMENT TRANSPORT AND DELIVERY ON THE LOWER TRINITY RIVER, TEXAS

Dr. Michael C. Slattery
Department of Geology
Texas Christian University
Fort Worth, Texas 76129

March, 2005

OVERVIEW

This report summarizes the work conducted during 2004-2005 under TWDB contract 2002-483-440. For this year, two subcontracts were signed: the first with Dr. Jonathan Phillips (*University of Kentucky*) who was charged with developing a sediment budget for the Galveston Bay system; the second with Dr. John Walden (*University of St. Andrews*) who, along with Dr. Mike Slattery, focused on assessing the potential of using mineral magnetic measurements to “fingerprint” sediment sources in the lower Trinity basin. Both reports are included in this document. It should be noted here, however, that suspended and bedload sampling in the Trinity and its two major downstream (i.e., below Lake Livingston) tributaries, namely Long King Creek and Menard Creek, are ongoing. The sediment rating curve for Romayor for 2002-2004 is now well developed (see Appendix 2 for current rating data), although the turbidity (and hence sediment discharge) record from September 2004 onward is still in storage in the probe, which remains submerged and inaccessible at current flow levels. The current rating curves for Long King Creek and Menard Creek are also included in Appendix 2, but the author feels it is still somewhat premature to submit final conclusions in relation to this data. These curves, and hence the current sediment transport regime, should be more fully quantified during year 5.

ENVIRONMENTAL MAGNETIC ANALYSIS OF SEDIMENT SAMPLES FROM THE TRINITY RIVER SYSTEM, TEXAS, USA.

INTRODUCTION

As part of an ongoing study of the geomorphological and sedimentological processes operating within the contemporary Trinity River system, Texas, USA, by Dr Mike Slattery (TCU) and Prof. Jonathan Philips (Kentucky), funded by the General Land Office/Texas Water Development Board, this report presents the results of an environmental magnetic study of potential source materials to the sediment system of the Trinity River and its sub-catchments.

The primary aim of this study was to evaluate the potential for using environmental magnetic analysis to characterise the sources and sediments of the Trinity River system with a view to using such characteristics to support ongoing work to understand the contributions made by the various sub-catchments to the overall sediment system. In order to use any compositional tool, including environmental magnetism, for establishing sediment-source linkages, measurable compositional variety is required. Within a fluvial system, any such variability needs to have some spatial order. In a system as large as that of the Trinity, the most obvious requirement is spatial variability on an inter-catchment basis – that is, the ideal circumstance would be for each major sub-catchment to deliver at its outlet a sediment whose compositional characteristics are distinct from the sediment to which they are being added.

The potential for this approach can be assessed in a number of different ways. However, for this work, the existence of a substantial pre-existing collection of sediment samples, taken from locations throughout many of the Trinity's sub-catchments, provided a cost-effective means of making an initial assessment. As a first stage, therefore, the work conducted here attempted to assess the variability of the potential sediment sources, both within and between individual sub-catchments. It was hoped that, on the basis of these data, the potential for using compositional data such as environmental magnetic measurements for studying sediment source-linkages could be evaluated.

ENVIRONMENTAL MAGNETISM

Environmental magnetic measurements were initially developed by palaeo- and rock magnetists as a means of identifying the assemblage of mineral species which were responsible for the preservation of any palaeomagnetic signal within a rock or sediment sample. Given that the information gained from this set of measurements was, in principle, similar in nature to the mineralogical information gained from quantitative applications of techniques such as X-ray diffraction techniques or petrological approaches such as thin section or heavy mineral analysis, these magnetic measurements found applications outside palaeomagnetic investigations.

Table 1 summarises the main applications of environmental magnetic analysis. As the methodology essentially provides the user with a compositional signal for the soil, sediment or rock under study, one of the most common applications of the technique has been for lithostratigraphic correlation and provenance indication.

Mineral magnetic analysis is now a commonly used form of sediment and rock analysis and has a number of distinct features (Thompson and Oldfield, 1986; Walden et al., 1999; Maher and Thompson, 1999; Evans and Heller, 2003):-

- i) The iron oxides which dominate the magnetic properties of most soils, sediments and rocks are both robust (persistent) and yet sensitive to a whole range of environmental processes. Although often present in very small amounts, they are rarely totally absent and, even in small amounts, can play an important role in the chemical behaviour of the material and dominate its colour.
- ii) Mineral magnetic instrumentation is very sensitive. For example, it can be several orders of magnitude more sensitive than XRD in terms of detection levels for iron oxide mineral concentrations.
- iii) Most magnetic measurements are non-destructive; magnetic measurements do not preclude other subsequent forms of analysis on the same samples.

Table 1 General applications of environmental magnetic analysis.

Application	Sedimentary environment	Example
Sediment correlation	Lacustrine, glacial, loess, fluvial, marine, soil erosion, etc.	Oldfield <i>et al.</i> (1985) Robinson (1982) Walden <i>et al.</i> (1996)
Sediment provenance	Lacustrine, glacial, loess, fluvial, marine, soil erosion, etc.	Oldfield <i>et al.</i> (1985) Smith <i>et al.</i> (1990) Walden <i>et al.</i> (1996) Walden <i>et al.</i> (1994) Walden <i>et al.</i> (1997) Slattery <i>et al.</i> (2000)
Weathering/soil forming processes	Contemporary soils, colluvial deposits, palaeosol identification, alluvial fan surfaces.	Maher (1986) Walden and Addison (1995)
Artificial tagging of sediment	Tracing movement of fluvial sediments.	Oldfield <i>et al.</i> (1981)
Pollution monitoring	Recent organic sediments, urban drainage, atmospheric pollution.	Hunt (1986)

Information concerning suspended sediment sources is an essential prerequisite in attempts to elucidate linkages within the sediment delivery system between the field and the river. One approach (e.g. Oldfield *et al.*, 1979; Walling *et al.*, 1979; Caitcheon, 1993; Walden *et al.*, 1997; Slattery *et al.*, 2000; Jenns *et al.*, 2002; Jenkins *et al.*, 2003) has involved the use of mineral magnetic analyses to provide a compositional fingerprint by which catchment sources can be compared with suspended sediments in order to investigate the likely sources for the latter.

In the context of attempts to quantify sediment source contributions using magnetic data, Lees (1994) summarised the prerequisites for successful 'unmixing' of sediment sources:

- i) Definition of potential source material types. It is critical to achieve optimal identification and definition of the source material properties as these represent the 'end members' of the model and strongly influence the eventual proportions of each source type ascribed to the sediment sample. This issue has a number of implications:
- ii) Field sampling needs to be organised appropriately to enable intra- and inter-source variation to be fully quantified (Lees, 1994).
- iii) Selection of the magnetic parameter values (e.g. mean) to represent each 'end-member' (source) is critical. Sensitivity of the model output to changes in the properties used to represent the sources should be considered to provide some idea of model reliability.
- iv) For successful modelling, the suspended sediment samples must have properties which lie wholly within the range of behaviour displayed by the values chosen to represent the sources. Errors in source definition, chemical alteration during transport or size selective transport of different sources may influence this.

The primary aim of the work undertaken here was to assess the viability of the magnetic approach for sediment-source linkages within the Trinity River system. The key first stage is, therefore, to establish the characteristics of the potential source materials. Our focus was therefore on issues (i) and (ii) above. Given the pre-existing sample database provided a reasonable spatial coverage of samples from throughout the system, fieldwork for (ii) concentrated on filling in particular areas within that sample framework. The subsequent environmental magnetic analysis performed on these samples was intended to address issue (i).

METHODOLOGY

All sample preparation and environmental magnetic analyses were carried out by JW within the Environmental Magnetism Laboratory of the Facility for Earth and Environmental Analysis (FEEA) located within the School of Geography & Geosciences, St Andrews University, U.K.

Sample preparation

Sub-samples of approximately 20g of the 138 samples available for mineral magnetic analysis were air dried at room temperature. Further sub-samples of c. 5-10 g were weighed (to 2 decimal places), the material wrapped in non-magnetic film and then packed in 10ml plastic pots and immobilised prior to analysis.

Analysis

A standard range of magnetic parameters were measured. Initial, low field, low frequency, mass specific, magnetic susceptibility (χ) was measured using a Bartington MS2 susceptibility meter.

The mass specific susceptibility to Anhysteretic Remanence Magnetisation (χ_{ARM}) was imparted by a Molspin A.F. demagnetiser with an ARM attachment. The χ_{ARM} created within the sample was measured using a Molspin 1A magnetometer.

The samples were then placed in a saturating field (1000 mT), created by a Molspin pulse magnetiser (capable of generating fields in the range 0-1000mT). The mass specific Saturation Isothermal Remanent Magnetisation (SIRM) created within the sample was measured using a Molspin 1A magnetometer.

The samples were then placed in successively larger reverse magnetic fields ('backfields'; opposite in direction to the initial saturating field) of 40, 100 and 300mT using the Molspin pulse magnetiser. After each field, the Isothermal Remanent Magnetisation (IRM) was measured using a Molspin 1A magnetometer.

Calculation and interpretation of mineral magnetic parameters

From the above measurements, four main magnetic parameters were calculated; χ , χ_{ARM} , SIRM and the 100 mT backfield ratio. Table 2 provides a basic interpretation of each of these parameters.

The majority of these parameters are sensitive to the concentrations of particular types magnetic minerals within a sample. For example, χ , for the majority of geological samples, be considered as a measure of the concentrations of ferrimagnetic type minerals (e.g. magnetite) within a sample. In contrast, SIRM is generally considered to be sensitive to the concentration of both ferrimagnetic (e.g. magnetite) and antiferromagnetic (e.g. haematite) type minerals. A number of other, less common parameters and inter-parametric ratios were also calculated (Table 2).

Table 2 Mineral magnetic parameters referred to in the text and their basic interpretation (after Dearing, 1999; Thompson and Oldfield, 1986; Maher, 1988; Oldfield, 1991; Walden *et al.*, 1999).

Parameter	Interpretation
χ ($10^{-8} \text{ m}^3 \text{ kg}^{-1}$)	Initial low field mass specific magnetic susceptibility. This is measured within a small magnetic field and is reversible (no remanence is induced). Its value is roughly proportional to the concentration of ferrimagnetic minerals within the sample, although in materials with little or no ferrimagnetic component and a relatively large antiferromagnetic component, the latter may dominate the signal.
χ_{ARM} ($10^{-8} \text{ m}^3 \text{ kg}^{-1}$)	Anhyseretic Remanent Magnetisation (ARM) is roughly proportional to the concentration of ferrimagnetic grains in the 0.02 to 0.4 μm (in the stable single domain size range). For this work ARM was induced in the samples using by combining a peak AF field of 100mT with a DC biasing field of 0.04mT and the final result expressed as mass specific ARM per unit of steady field, χ_{ARM} (Maher, 1988).
SIRM ($10^{-5} \text{ Am}^2 \text{ kg}^{-1}$)	Saturation isothermal remanent magnetisation is the highest amount of magnetic remanence that can be produced in a sample by applying a large magnetic field. It is measured on a mass specific basis. In this study a 'saturating' field of 1T has been used and this will produce saturation in most mineral types. However, some antiferromagnetic minerals may not be saturated at this field (e.g. goethite) and therefore this parameter is often called IRM _{1T} . The value of SIRM is related to concentrations of all remanence-carrying minerals in the sample but is also dependent upon the assemblage of mineral types and their magnetic grain size.
Soft IRM ($10^{-5} \text{ Am}^2 \text{ kg}^{-1}$)	Based upon the amount of remanence lost by a saturated sample after experiencing a backfield of 40mT. At such low fields, the magnetically 'hard' (high coercivity) canted-antiferromagnetic minerals such as haematite or goethite are unlikely to contribute to the IRM, even at fine grain sizes. The value is therefore approximately proportional to the concentration of the magnetically 'softer' (low coercivity) ferrimagnetic minerals (e.g. magnetite) within the sample, although also grain size dependent.
Hard IRM ($10^{-5} \text{ Am}^2 \text{ kg}^{-1}$)	Based upon the amount of remanence remaining in a saturated sample after experiencing a backfield of 300mT. At fields of 300mT, the majority of magnetically 'soft' (low coercivity) ferrimagnetic minerals will already have saturated and any subsequent growth of IRM will be due to a magnetically 'harder' (high coercivity) canted antiferromagnetic component within the sample. The value is therefore approximately proportional to the concentration of canted antiferromagnetic minerals (e.g. haematite and goethite) within the sample.
IRM Backfield Ratios	Various magnetisation parameters can be obtained by applying one or more magnetic fields to a sample. The magnetisation at each backfield can be expressed as a ratio of IRM _{field} /SIRM, and therefore gives a result between +1 and - 1, normalised for concentration. Such ratios can be used to discriminate between ferrimagnetic and canted antiferromagnetic mineral types. For example, using the 100mT backfield ratio, minerals which are relatively easy to demagnetise (e.g. magnetite) have relatively low values (-ve values; referred to as 'soft' (low coercivity) magnetic behaviour). Minerals which show a stronger resistance to demagnetisation (e.g. haematite) show relatively high 100mT backfield ratios (positive or near zero values; referred to as 'hard' (high coercivity) magnetic behaviour).

RESULTS

Summary data for full sample set

A full set of the magnetic data obtained for the 138 samples analysed here is contained in Appendix 1. Summary data are provided in Tables 3 and Fig. 1.

Table 3 Summary data for 138 source sediment samples from the Trinity River basin system. Basic interpretations and units for each parameter are shown in Table 2.

	χ_{lf}	χ_{arm}	SIRM	χ/χ_{arm}	SIRM/ χ	Soft IRM	Hard IRM	-40 mT	-100 mT	-300 mT
Mean	12.07	6.29	195.27	2.45	26.33	115.58	31.84	0.03	-0.48	-0.73
St Dev	21.49	16.39	677.44	2.00	50.57	483.56	123.79	0.25	0.25	0.23
Min	-0.10	0.88	7.19	-0.07	2.73	2.51	0.39	-0.63	-0.89	-1.00
Lower Quartile	5.25	2.21	39.72	1.38	12.89	17.18	3.57	-0.13	-0.59	-0.82
Median	7.75	3.41	56.32	2.12	16.79	25.04	5.57	0.09	-0.52	-0.79
Upper Quartile	10.65	4.62	103.61	3.06	25.71	44.43	11.93	0.16	-0.43	-0.69
Max	210.20	168.89	6986.19	16.77	559.51	5058.90	965.30	0.99	0.96	0.76

These summary data show that all magnetic variables display significant variability within the complete sample set. For example, the most basic concentration-dependent magnetic parameter, magnetic susceptibility (χ_{lf}), shows values ranging between -0.10 (typical of diamagnetic behaviour) to 210.20 (stronger than that found in most sedimentary rocks but not untypical of top-soils or metamorphic/igneous rocks – Dearing, 1999). However, as demonstrated by the upper and lower quartile values (and the shaded boxes in Fig. 1 which mark the positions of the upper and lower quartiles for each parameter), the majority of the samples are contained within a much smaller range (5.25 to 10.65) and at values that are more typical of sedimentary rocks or soils developed upon them.

This same pattern is seen in the other concentration-dependent magnetic parameters (χ_{arm} , SIRM, Soft IRM and Hard IRM); while a small number of samples show extremely high values, suggesting high concentrations of magnetic minerals in those particular samples, the bulk of the samples show values that lie within a much smaller range. For example, 75% of the samples have χ_{arm} values less than 4.62. This suggests that ultra-fine magnetic minerals are not present in significant quantities within the majority of the samples analysed here. Equally, 75% of all SIRM values are less than 103.61, suggesting that the majority of the samples are dominated by medium to low overall concentrations of magnetic minerals. This is again consistent with values found in many sedimentary rocks or the soils developed upon them.

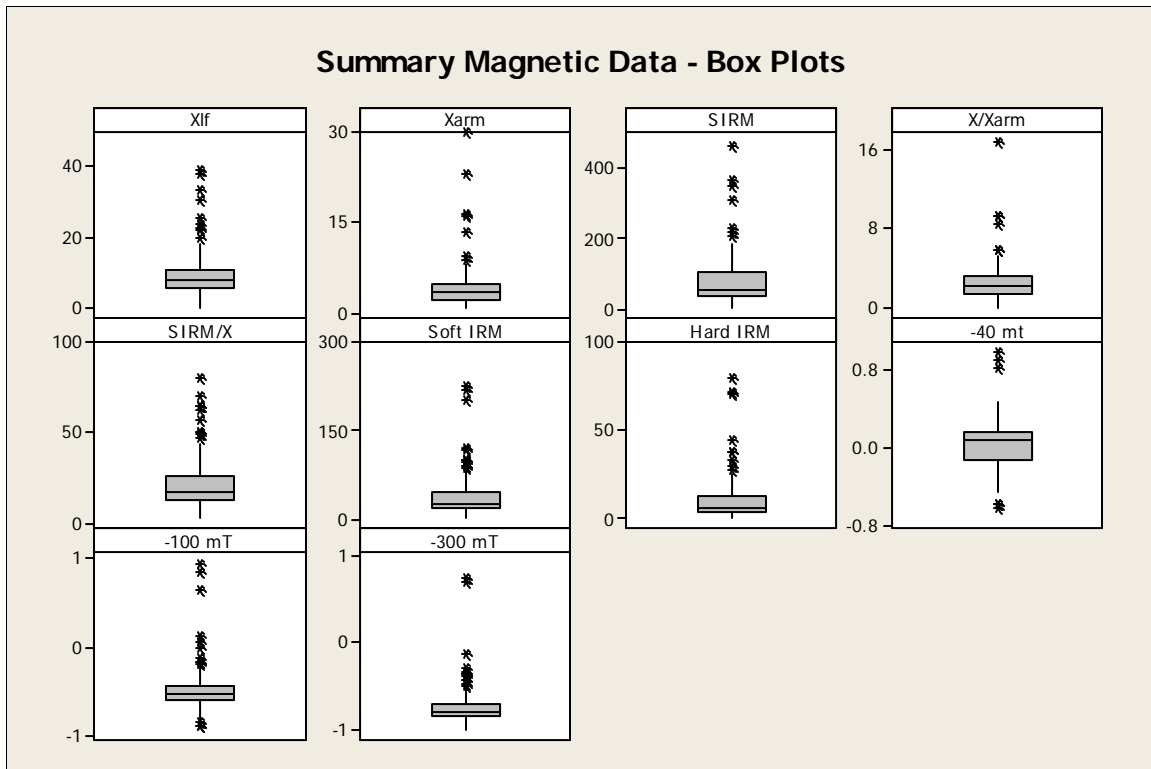


Fig. 1 Box plots for each magnetic variable. Plot shows median, upper and lower quartiles and outlying extreme values. Note that for all concentration parameters, maximum values have been excluded to enable detail of the data distributions to be seen.

As indicated in Table 2, Soft IRM and Hard IRM are indicative of the concentrations of low coercivity (e.g. magnetite) and high coercivity (e.g. haematite, goethite) magnetic minerals respectively. Per unit mass, the remanence behaviour of magnetite is several orders of magnitude greater than that of haematite or goethite. The dominance of relatively low Soft IRM values and what are moderate Hard IRM values suggests a mixed magnetic assemblage, with, mass for mass, high coercivity mineral types dominating.

As they are normalised for magnetic concentration, the three backfield ratios (measured at -40, -100 and -300 mT) are also useful indicators of the mixture of low and high coercivity behaviour within the samples. The median -100 mT ratio value of -0.52 is consistent with the observation made above about the mixed magnetic assemblage – in a sample set containing a majority of low coercivity minerals such as magnetite, values between -0.8 and -1.0 would be dominant. The higher values found here indicate a significant contribution from higher coercivity mineral types such as haematite or goethite.

Catchment-specific data

Given the context of this work, consideration of the data on a catchment-specific basis is clearly of interest. While a number of samples lie on or close by the main Trinity River channel, some 64 of the 138 samples are located in four distinct areas and these serve as a suitable sub-set to consider the degree of inter- and intra-catchment variability in the source material magnetic properties. Three sub-catchments (Big Thicket (part of Menard Creek), Sam Houston National Forest (part of Big Creek) and Polk County Uplands (part of upper Long King Creek)) feeding the Trinity between Lake Livingston Reservoir and Romayor make for an interesting comparison with samples collected near the systems outlet on the Trinity River Delta. Summary data for these four sub-sets of samples are provided in Table 4.

Table 3 Median values of the main magnetic parameters for selected sub-sets of source sediment samples from the Trinity River basin system. Basic interpretations and units for each parameter are shown in Table 2.

	n	χ_{lr}	χ_{arm}	SIRM	χ/χ_a r_m	SIR M/ χ	Soft IRM	Hard IRM	-40 mT	-100 mT	-300 mT
Trinity River Delta (TRD)	17	6.40	3.86	40.84	1.66	15.06	19.42	4.00	0.12	0.54	-0.82
Big Thicket (BT)	6	19.35	6.21	316.79	2.33	37.91	80.62	44.13	-0.22	0.58	-0.70
Sam Houston National Forest (SHNF)	7	33.10	23.07	968.91	1.93	49.04	771.3 5	155.62	-0.41	0.58	-0.82
Polk County Uplands (PCU)	15	11.00	3.64	115.94	3.17	28.96	53.63	19.06	0.07	0.47	-0.74

A number of features can be highlighted from Table 3. First, for all the concentration-dependent magnetic parameters, the Trinity River Delta (TRD) samples show lower magnetic concentrations than any of the three sub-catchment sets. The median properties of the Polk County Uplands (PCU) samples are closest to the TRD median values in terms of both concentration-dependent (e.g. SIRM) and mineralogical (e.g. -40 mT backfield ratio) parameters. In contrast, the highest magnetic concentrations are found in the Sam Houston National Forest (SHNF) sub-set.

Figures 2-5 show boxplots for a selection of the magnetic parameters and confirm these observations. Within the limitations posed by the relatively small sample sets for both BT and SHNF, it would appear that both of these sub-catchments contain potential sources with very high concentrations of magnetic minerals. For example, even with the relatively small sample sets available here, differences between the SHNF sub-set and the TRD sub-set are statistically significant for χ_{lr} , SIRM and Hard IRM. Similarly, differences between the SHNF and PCU sub-sets are statistically significant for SIRM and Hard IRM.

While both the SHNF and BT sub-sets show the highest concentrations of magnetic minerals, they also show considerably greater compositional variability than either the TRD or PCU sub-sets. This may, in part, be a reflection of the small sample numbers involved. However, it also demonstrates that source material composition within a single sub-catchment can be quite large. This would be expected given the overall size of the field area and the various sub-catchments within it, but it does suggest relatively large numbers of samples are needed to be confident that potential source variability has been accurately assessed in any particular sub-catchment within the overall system.

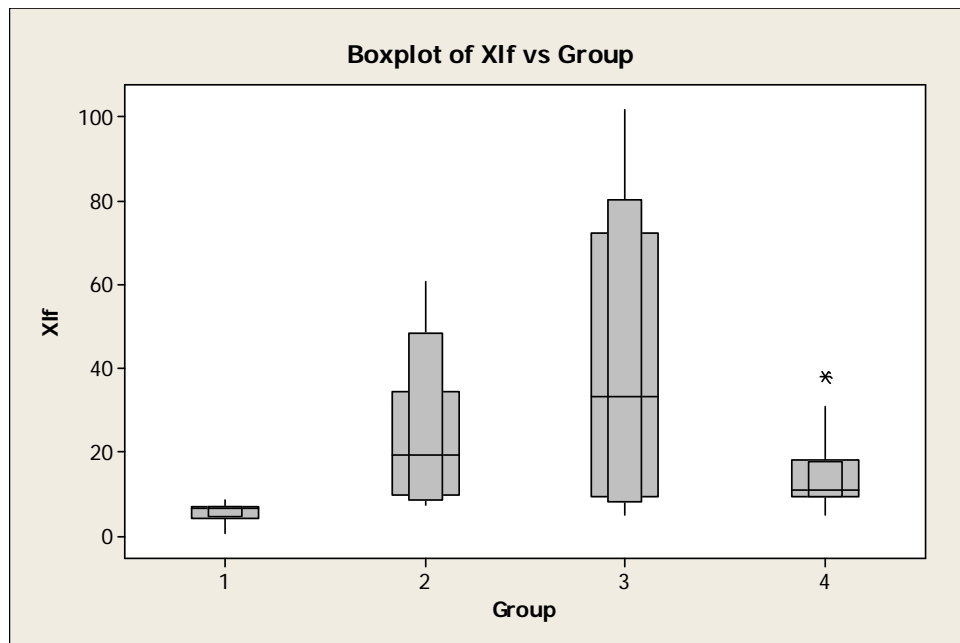


Fig. 2 Box plots for χ_{if} for each of the four sample sub-sets described in the main text. Plot shows median, upper and lower quartiles and outlying extreme values. The narrower 'inner-box' represents a 95% confidence interval around the median. Where these confidence intervals do not overlap, the respective medians can be assumed to be statistically different at the 95% confidence level. Groups are 1=TRD, 2=BT, 3=SHNF, 4=PCU.

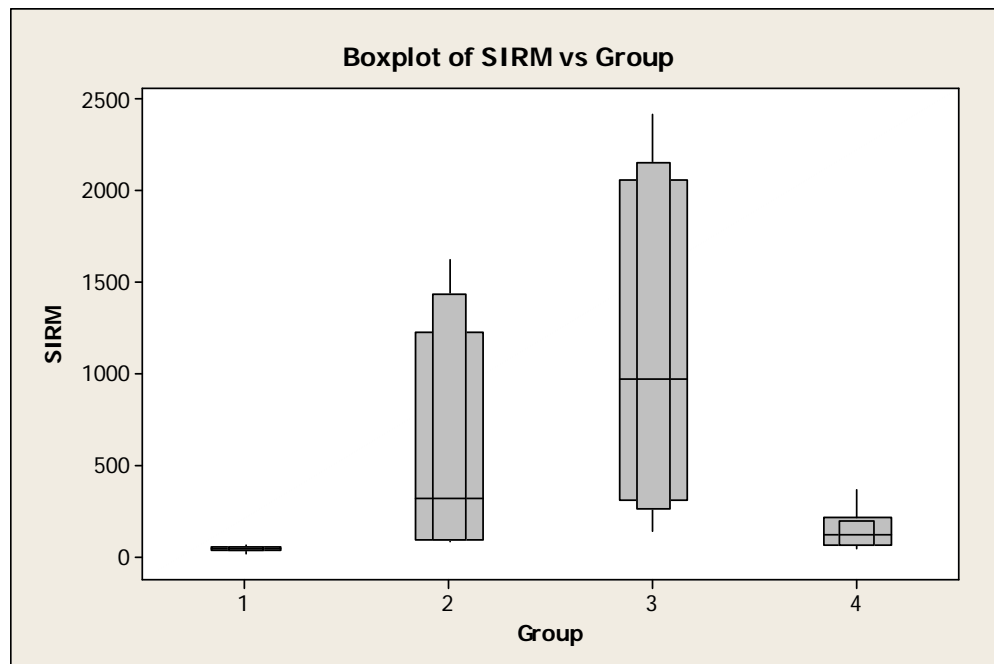


Fig. 3 Box plots for SIRM for each of the four sample sub-sets described in the main text. Details as in Fig. 2.

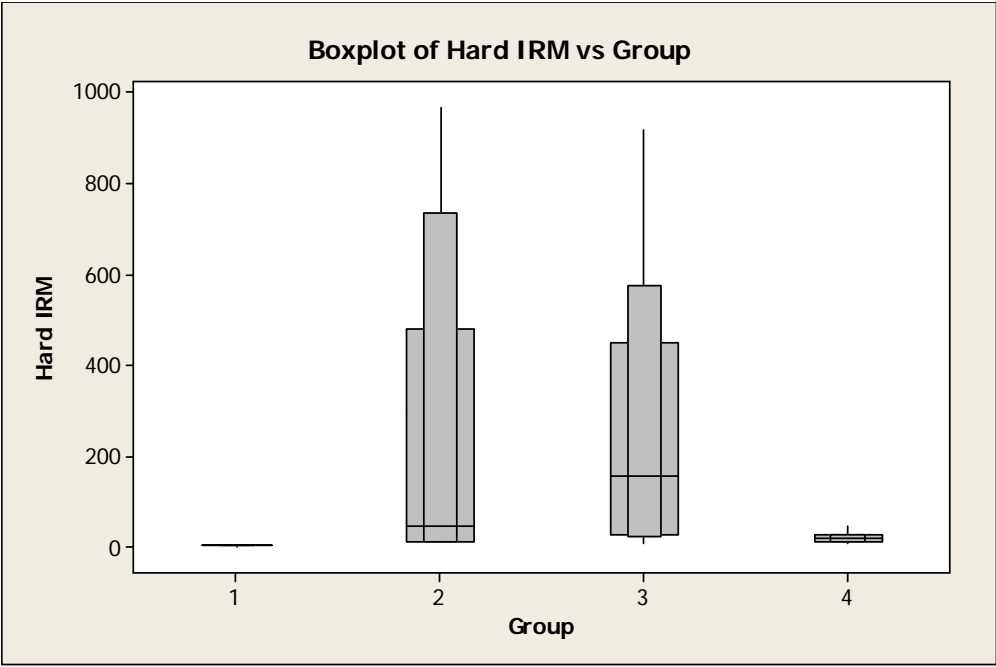


Fig. 4 Box plots for Hard IRM for each of the four sample sub-sets described in the main text. Details as in Fig. 2.

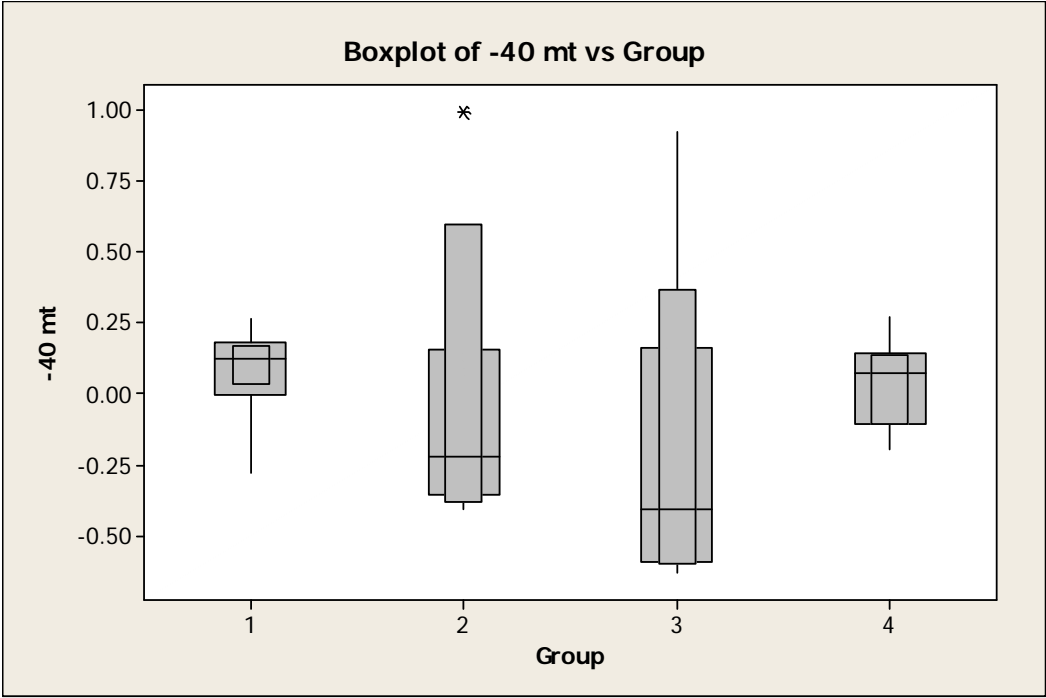


Fig. 5 Box plots for -40mT backfield ratio for each of the four sample sub-sets described in the main text. Details as in Fig. 2.

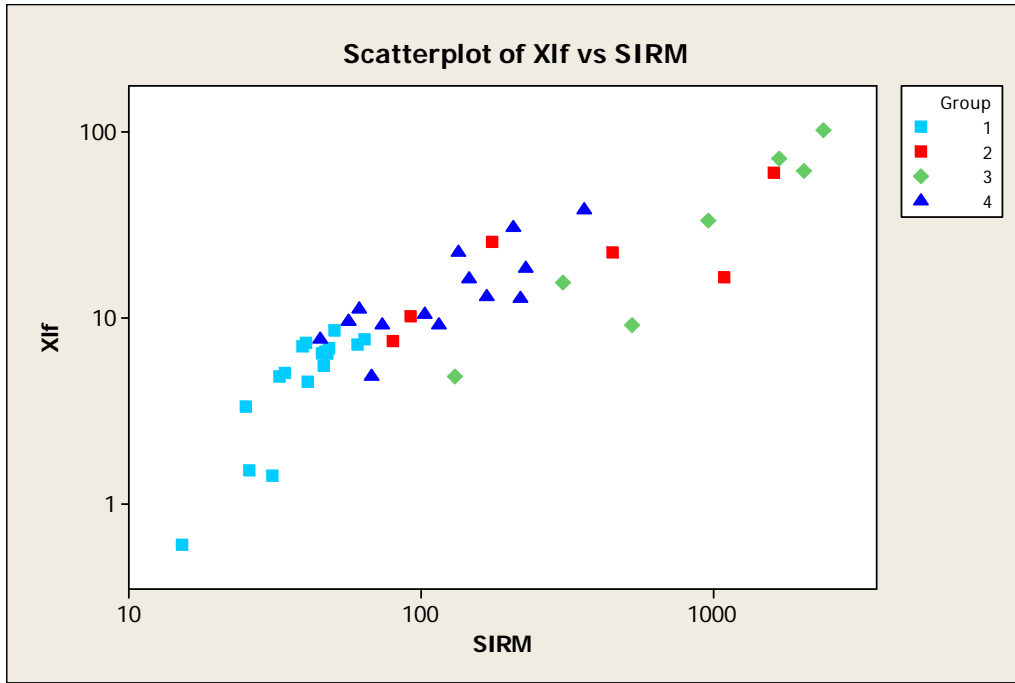


Fig. 6 Bi-plot of χ_{if} vs SIRM for each of the four sample sub-sets described in the main text. Groups are 1=TRD, 2=BT, 3=SHNF, 4=PCU.

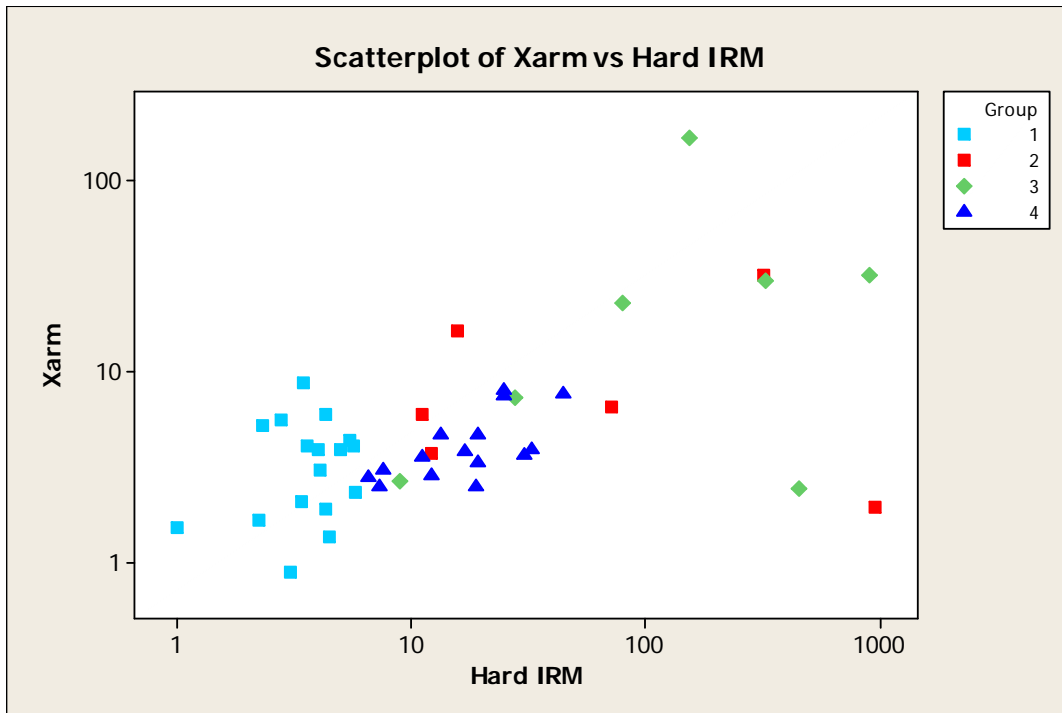


Fig. 7 Bi-plot of χ_{arm} vs Hard IRM for each of the four sample sub-sets described in the main text. Groups are 1=TRD, 2=BT, 3=SHNF, 4=PCU.

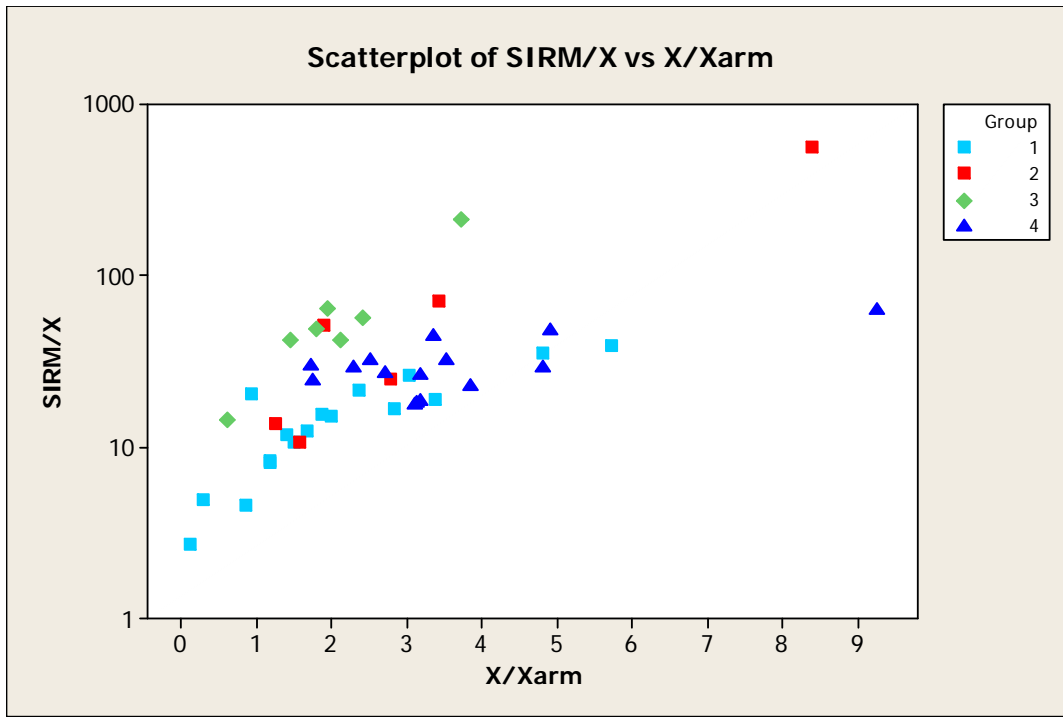


Fig. 8 Bi-plot of $SIRM/\chi_{arm}$ vs χ/χ_{arm} for each of the four sample sub-sets described in the main text. Groups are 1=TRD, 2=BT, 3=SHNF, 4=PCU.

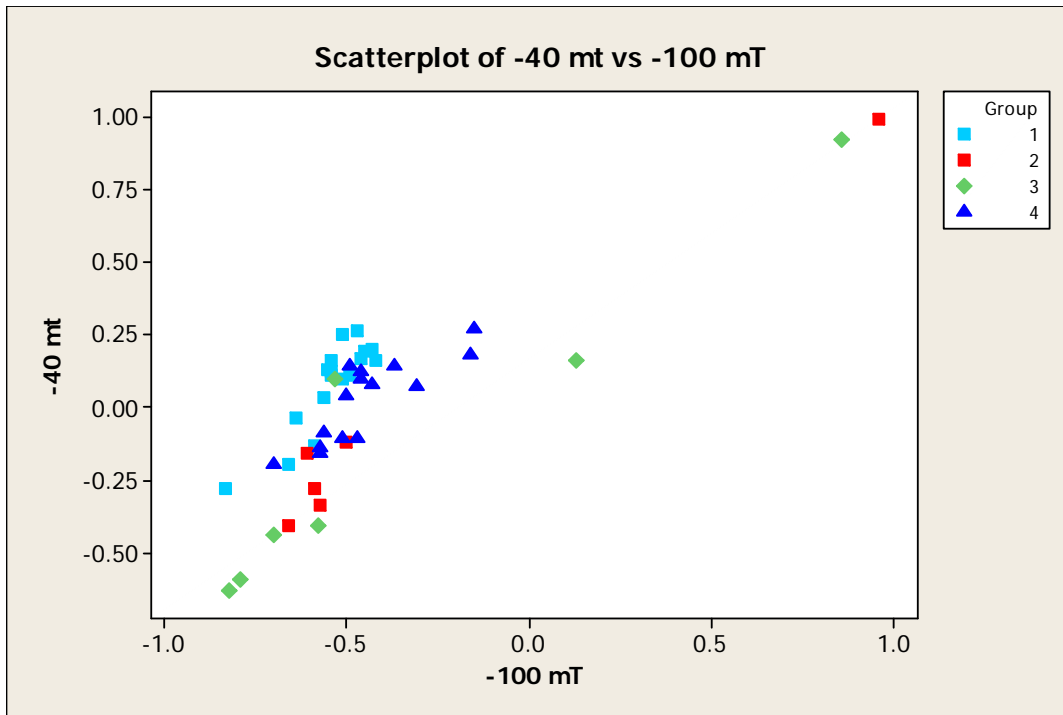


Fig. 9 Bi-plot of the -40mT vs -100mT backfield ratios for each of the four sample sub-sets described in the main text. Groups are 1=TRD, 2=BT, 3=SHNF, 4=PCU.

Bi-plots (Figs 6 to 9) illustrate both these inter-catchment and intra-catchment differences in the basic magnetic properties of the four sample sub-sets. Notice that in each case, while there is overlap between each of the four sample sub-sets, clear grouping does exist demonstrating a degree of inter-unit (between catchment) variation. However, intra-unit (within catchment) variation is also present and, in the case of the BT and SHNF sub-sets, some samples show extreme magnetic behaviour (note the log scale used in some of the plots) relative to the majority of the samples analysed here.

Multivariate statistical analysis

A wide range of analytical techniques commonly used within geological/environmental research projects produce multivariate data sets. In addition, many such research projects are of a multidisciplinary nature. Thus a typical data set may consist of a number of geological field samples (sediments or soils) for which, for example, mineralogy, elemental chemistry and fossil content (by pollen analysis) have been measured. The data matrix of n samples by m variables can therefore become quite large.

Although many cases will exist where clear patterns emerge from such data sets, often, where the relationships within the data are more complex or subtle, a purely subjective interpretation may not be suitable, and the researcher faces the problem of how to compare the respective properties of groups of samples in order to improve understanding of the environmental context from which the samples came. Although this can be done objectively on a simple, univariate basis, such an approach gives no impression of how sample sets respond to groups of variables simultaneously. The problem faced is trying to understand how the n samples are arranged relative to all m variables together (that is, which samples plot close together in m -dimensional space?) It would be preferable if a multivariate technique could be adopted.

In some cases, such problems can be tackled by applying simultaneous R- and Q-mode factor analysis. Factor analysis has been used in various branches of geology and seems to offer a useful means for exploration of multivariate relationships within suitable data sets (Davis, 2002). While you may start with m -dimensions (variables), the factor analysis attempts to reduce the dimensionality of the problem by looking for the underlying trends within the data (for example, by establishing if several variables are highly correlated).

The environmental magnetic data for all 138 source samples was therefore subjected to a factor analysis using the method outlined in Walden *et al.* (1992). This was performed in MINITAB v. 14. Fig 10 shows a scree plot of the eigenvalues for the factors extracted. The high eigenvalues for factors 1 and 2 (3.9 and 3.6 respectively) suggest that together, factors 1 and 2 explain approximately 75% of the variability contained within the original 10 magnetic variables used in the analysis – that is, a plot of the sample loadings for factors 1 and 2 should, within a two-dimensional plot, contain 75% of the information within the full, ten-dimensional data set. The other factors are of considerably less importance.

Fig. 11 shows the variable loadings for factors 1 and 2 and illustrates the positions of the original variables in relation to the factors extracted. As can be seen, relative to the origin, factor 1 is dominated by χ_{lf} , χ_{arm} , SIRM and Soft IRM, all of which produce strong negative loadings on Factor 1. All these parameters are sensitive to the concentration of low coercivity magnetic minerals. Therefore, the most obvious interpretation of this factor is as an indicator of magnetite concentration, with greater concentrations indicated by more negative loadings.

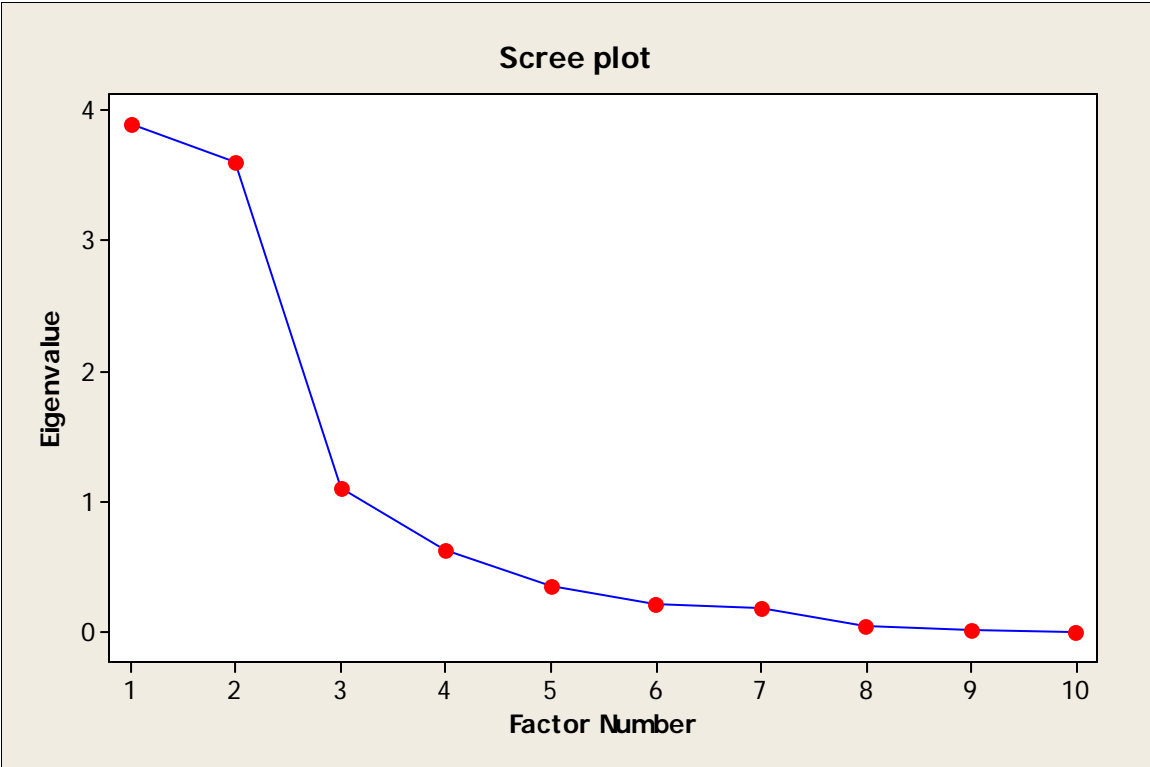


Fig. 10 Scree plot of eigenvalues for the factors extracted from the R- and Q-mode factor analysis.

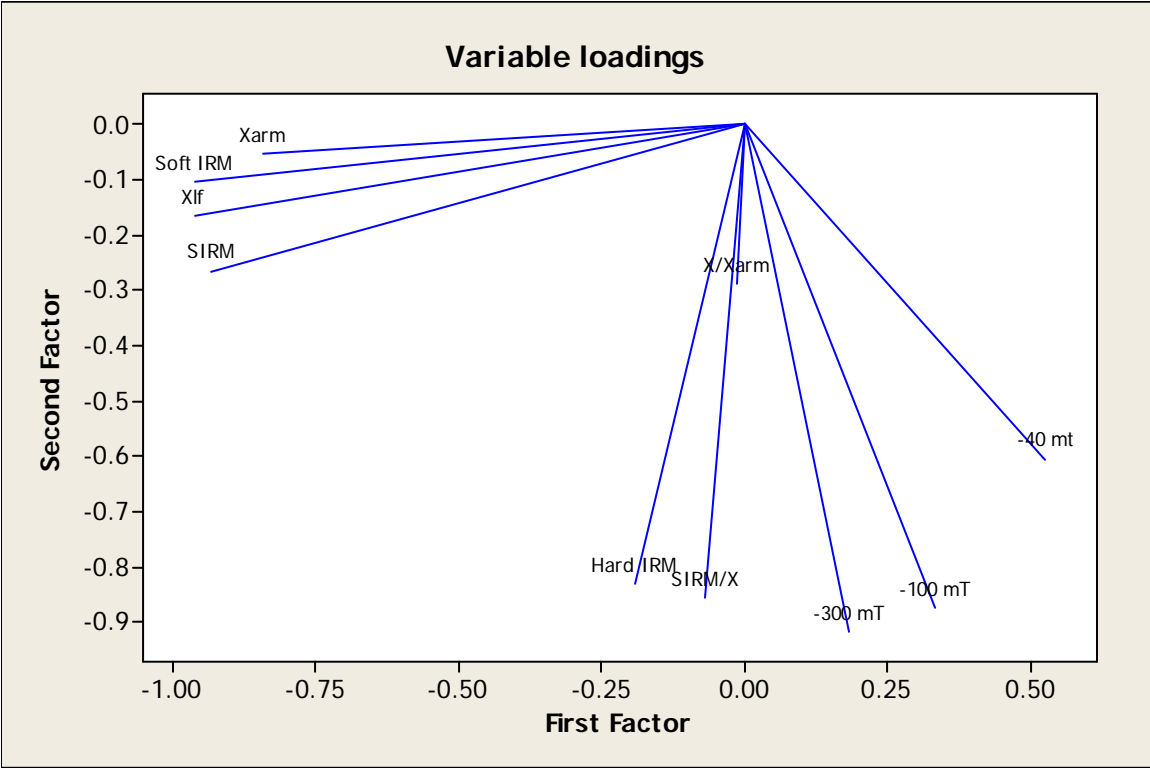


Fig. 11 Variable loadings for factors 1 and 2 extracted from the R- and Q-mode factor analysis.

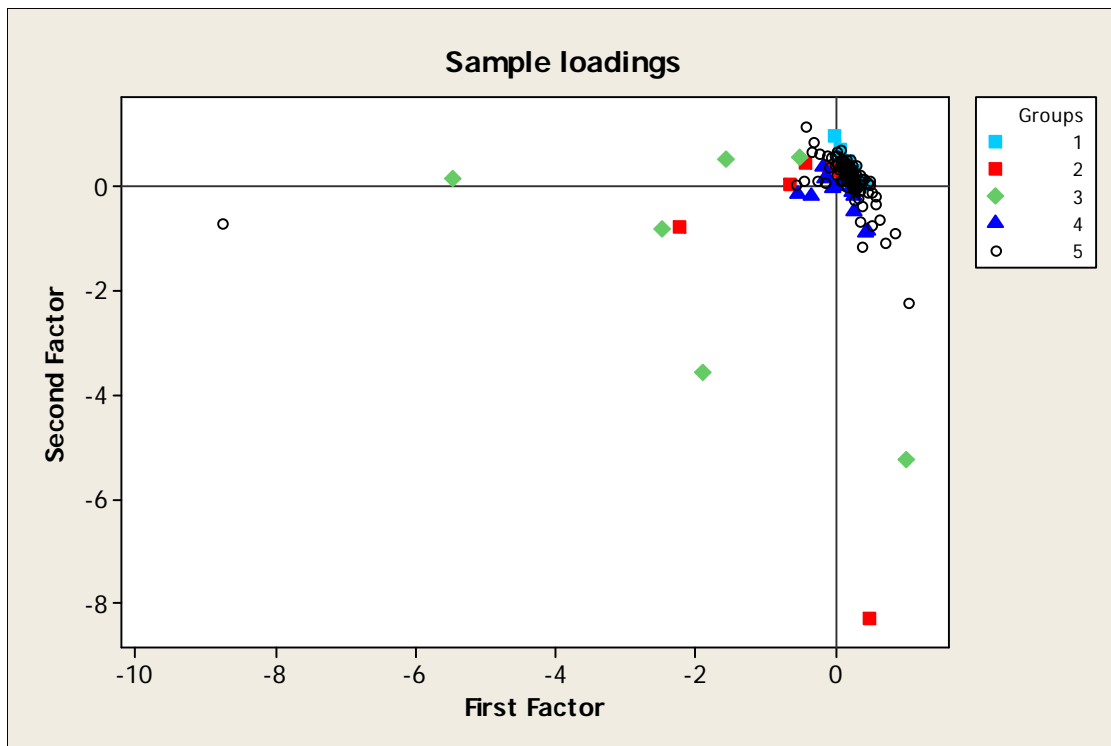


Fig. 12 Sample loadings for factors 1 and 2 extracted from the R- and Q-mode factor analysis. Groups are 1=TRD, 2=BT, 3=SHNF, 4=PCU, 5=all other samples.

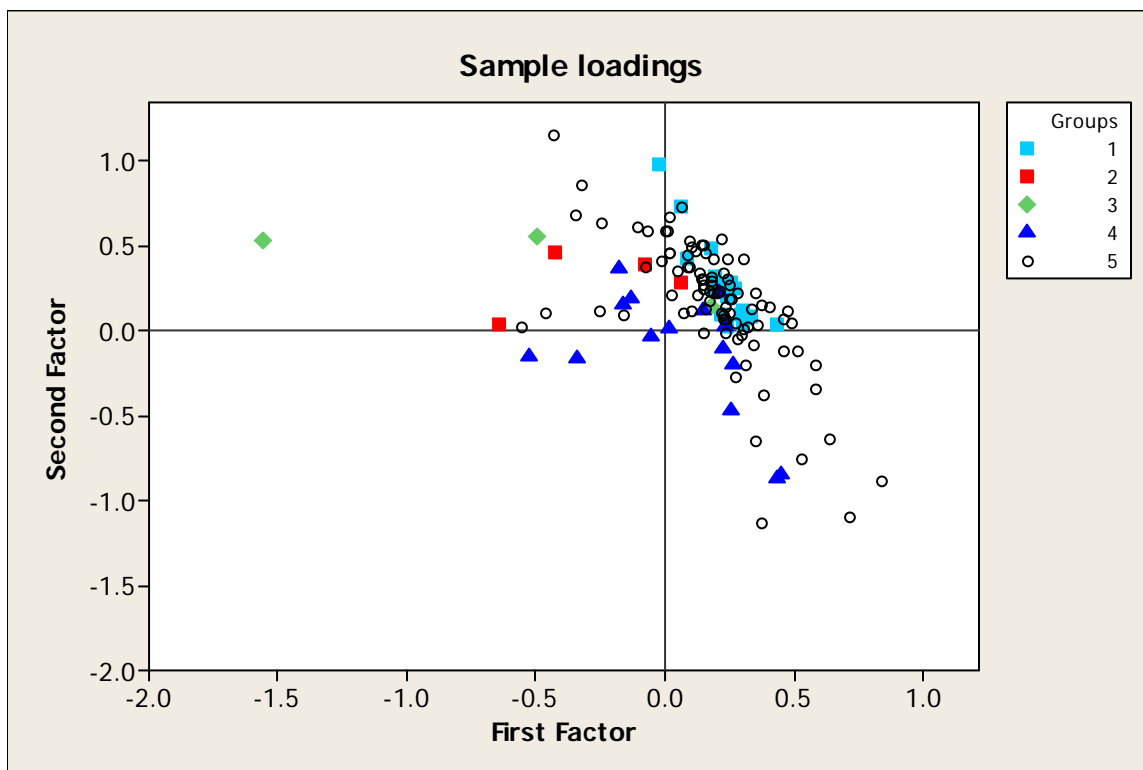


Fig. 13 Inset from Fig. 12 showing detail of sample loadings for factors 1 and 2 extracted from the R- and Q-mode factor analysis. Groups are 1=TRD, 2=BT, 3=SHNF, 4=PCU, 5=all other samples.

In contrast, factor 2 is dominated by those magnetic parameters that are more sensitive to mineral type as opposed to concentration. Again, these variables show negative loadings, suggesting high values of the original variables will result in strongly negative loadings on factor 2. Factor 2 can therefore be considered as responding to both the concentration of high coercivity minerals such as haematite (high Hard IRM values) and the balance between the mixture of low and high coercivity mineral types (e.g. the -100 mT backfield ratio), with more negative loadings indicating greater proportions on high coercivity minerals.

Figure 12 shows the sample loadings for factors 1 and 2 with Fig. 13 providing an inset to allow the detail of the area where the majority of the samples plot within Fig. 12. The extreme nature of the SHNF sample magnetic properties are clearly demonstrated, although this small sample group does considerable intra-group variability. The BT samples are shown to be distinct from the majority of the remaining samples with relatively negative factor 1 loadings (consistent with the high magnetic concentrations seen in the raw data for these samples). Interestingly, the PCU samples seem to fall into two groups – one showing negative factor 1 loadings (suggesting higher magnetic concentrations) and one showing negative factor 2 loadings (suggesting a greater proportion of high coercivity mineral types). Again, this suggests clear intra-group compositional variability within samples from a single sub-catchment.

Figure 13 shows that the TRD samples are fairly tightly grouped (relatively low levels of intra-group variability) and appear to plot with little overlap to the BT, SHNF and PCU sample sets, demonstrating clear inter-group variability. The remainder of the samples from the full sample set seem to occupy the same factor space as the TRD, BT and PCU samples with only one sample showing extreme magnetic behaviour similar to that seen in the SHNF sub-set.

DISCUSSION

The results presented in section 4 demonstrate considerable variability in the magnetic properties of the various source samples analysed (and, by inference, their iron mineral composition). The majority of the samples analysed display relative low concentrations of low coercivity minerals such as magnetite (e.g. low χ_{lf} values). Mixed magnetic mineral assemblages, with significant proportions of high coercivity minerals such as haematite or goethite are dominant (relatively high Hard IRM values and high -100 mT backfield ratios). Low χ_{arm} values suggest little contribution from ultra-fine-grained magnetic minerals. This type of magnetic behaviour is not untypical of many sedimentary rocks or the soils developed upon them. A small number of 138 samples do display more extreme magnetic behaviour, manifested by higher concentrations of magnetic minerals and, in particular, low coercivity minerals such as magnetite.

When considered on a catchment-basis, the overall magnetic properties of certain sub-catchments do appear to show distinct magnetic properties. This is seen clearly with catchments such as Sam Houston National Forest (SHNF), where the strong magnetic properties of some of the potential source samples demonstrate high concentrations of magnetic minerals. However, even in those catchments such as Big Thicket (BT) or areas of the Trinity River Delta (TRD), where lower magnetic mineral concentrations dominate, sub-catchments to appear to show distinct magnetic properties that, when considered on a multivariate basis, can generally be differentiated.

The ability to identify such inter-catchment variability is an essential pre-requisite if any compositional methodology, including environmental magnetic analysis, is to have potential for linking catchment sources to the sediment being transported within the Trinity River system. Given these preliminary results, it may well be possible to use the magnetic characteristics of sediments supplied from a sub-catchment to identify their potential contribution to sediment system within the main river system immediately downstream of the sub-catchment outlet.

However, this statement needs to be qualified by two limitations presented by these data.

- i) As illustrated by the factor analysis output (Figs 12 and 13), the potential source samples for some of the sub-catchments show either (a) similar properties to each other or (b) high levels of intra-group compositional variability within the sub-catchment. Both of these features would make any subsequent studies of their source-sediment linkages more problematic.
- ii) The considerable compositional variability demonstrated by the potential source materials within sub-catchments such as SHNF and BT suggest that fully characterising the magnetic properties of the major sub-catchments within the overall system would require large numbers of samples in order to ensure that (a) the diverse nature of the potential sources was fully represented; (b) that the spatial distribution of each potential source within a sub-catchment is established; (c) that the properties of those areas most likely to contribute to the sediment system (e.g. channel banks) are fully quantified.

Given the size of the Trinity River system and its many sub-catchments, fully characterising the magnetic properties of each potential major sediment source in the fashion piloted in this study would represent a significant undertaking. This would require a further investigation to more fully establish the level of spatial variability of potential sources in order to develop a reliable sampling strategy and thus ensure that the magnetic properties of each source are accurately quantified.

An alternative approach, based on the method of Caitcheon (1993), may prove more efficient. This procedure concentrates upon characterising the suspended sediment both up-stream and down-stream of major tributaries. In the most straight-forward case, where a sub-catchment joins a main channel, the suspended sediment is characterised at three points:-

- i) Within the main channel up-stream of the tributary (end-member 1).
- ii) Within the main channel of the sub-catchment up-stream of where it joins the main channel (end-member 2).
- iii) Within the main channel down-stream of the tributary (the resulting mix of end-members 1 and 2).

For the purposes of modelling and/or quantifying the contribution made by the sub-catchment to the main channel sediment system, in principle, this approach is conceptually simple. The compositional properties of the two 'end-members' can be used to provide a means by which their relative contributions to the resulting mix can be established.

This approach avoids the issue of the inherent variability of the various sources within each sub-catchment by concentrating upon the properties of the actual sediment delivered to the sub-catchment outlet. The method is not, however, without its own difficulties. Two of these are methodological and would apply in any catchment system. First, it is essential that the compositional properties of the two 'end-members' at any tributary junction can be distinguished in some fashion. Second, the analysis requires the collection of suspended sediment samples. While these samples do not have to be collected continuously, in ideal circumstances, samples representative of both low and high flow conditions should be analysed. Different flow regimes may be acquiring sediments from different source areas within the sub-catchment and, until demonstrated otherwise, it should not be assumed that their magnetic properties are identical.

The third difficulty here concerns the scale of the Trinity River system itself. Given the large spatial area and the considerable number of sub-catchments present, some compromise may be required if this alternative approach was to be attempted. Grouping of sub-catchments would reduce the effort required to collect the necessary suspended sediment samples but would also reduce the spatial resolution possible when identifying major suppliers of sediment sources.

Given these observations, any future attempts to use compositional properties to establish sediment-source linkages within the Trinity River system, or efforts to quantify the relative contributions of the various sub-catchments to the overall sediment budget of the system, should be preceded by a further evaluation programme. Ideally, this should involve two sub-catchments of different magnetic characteristics – one with high concentration of magnetic minerals and another with low/intermediate concentrations. In each case, this should involve a suspended sediment sampling programme both upstream and downstream of the sub-catchment tributary, although this would not necessarily need to be continuous sampling, with a view to characterising the compositions of the sediments. Such an evaluation programme could establish the feasibility of a sediment source mixing model based on environmental magnetic properties for ascribing the contribution to the main channel sediment transport system made by the respective sub-catchments.

CONCLUSIONS AND RECOMMENDATIONS

Conclusions

The main conclusions drawn in this work are as follows:-

- i) Environmental magnetic analysis of 138 potential catchment source samples from within the Trinity River system shows a dominance of samples containing relatively low concentrations of magnetic minerals, with mixed assemblages of low and high coercivity mineral types present.
- ii) A smaller number of samples show more extreme magnetic behaviour, showing higher concentrations of magnetic minerals and, in particular, higher concentrations of low coercivity minerals such as magnetite.
- iii) When analysed at the level of a sub-catchment, the data show a measurable level of inter-catchment variability. This suggests that there is potential for using environmental magnetic measurements as a means of evaluating source contributions to the sediment system within the Trinity River system.
- iv) For some sub-catchments, however, the magnetic data also shows considerable levels of intra-catchment variability. In order to fully quantify this variability to ensure the accuracy of any quantitative sediment-source ascription, extensive field sampling of likely sources would be required.

Recommendations

Given the above conclusions, the following recommendations are made from this work:-

- i) While these data suggest that quantitative sediment contribution estimates from the various sub-catchments of the Trinity River system may be possible, the large scale of the system and the inherent spatial variability of the potential source materials at the sub-catchment level suggest that such an approach would be a significant undertaking. In addition to collection of active sediment samples from within the channel system (the compositional 'target' that would be unmixed in terms of the potential sources), characterising the multitude of potential sources would require extensive and rigorous field sampling.
- ii) A more pragmatic approach would involve the methodology adopted by Caitcheon (1993), whereby the sediments in transport up-stream of a major tributary are used as end-members to unmix the composition of the sediments in transport down-stream of the tributary.
- iii) While the approach under (ii) is more likely to be effective than one based upon characterising potential sources from within the catchment, in a system as large as the Trinity River, it would still require significant resources to fully implement. If this approach is thought worthy of pursuing, therefore, a further evaluative study would be recommended. Ideally, this should involve two sub-catchments of different magnetic characteristics – one with high concentration of magnetic minerals and another with low/intermediate concentrations. In each case, this should involve a suspended sediment sampling programme both upstream and downstream of the sub-catchment tributary, although this would not necessarily need to be continuous sampling, with a view to characterising the compositions of the sediments. Such an evaluation programme could establish the feasibility of a sediment source mixing model based on environmental magnetic properties for ascribing the contribution to the main channel sediment transport system made by the respective sub-catchments.

REFERENCES

- Caitcheon, G. G. 1993. Sediment source tracing using environmental magnetism: a new approach with examples from Australia. *Hydrological Processes*, 7, 349-358.
- Davis, J.C., 2002. Statistics and data analysis in geology. 3rd edition, Wiley, New York.
- Dearing J. 1999. Magnetic Susceptibility. In *Environmental Magnetism, A Practical Guide*, Walden J, Smith JP, Oldfield F (Editors). Quaternary Research Association. Technical Guide No.6; 35-62.
- M.E. Evans and F. Heller, 2003. Environmental magnetism: principles and applications of enviromagnetics, Academic Press, Amsterdam, 299 pp.
- Hunt, A. 1986. The application of mineral magnetic methods to atmospheric aerosol discrimination. *Physics of Earth and Planetary Interiors*, 42, 10-21.
- Jenkins, P., Duck, R.W., Rowan, R.S. and Walden, J. 2003. Fingerprinting of bed sediment in the Tay Estuary, Scotland: An environmental magnetism approach, *Hydrology and Earth System Science*, 6, 1007-1016.
- Jenns, N., Heppell, K., Burt, T., Walden, J. and Foster, I.D.L. 2002. Investigating contemporary and historical sediment inputs to Slapton Higher Ley: an analysis of the robustness of source ascription methodology when applied to lake sediment data. *Hydrological Processes*, 16, 3467-3486.
- Lees, J. A. 1994. *Modelling the magnetic properties of natural and environmental materials*. Unpublished PhD thesis, Coventry University.
- Maher, B. A. 1986. Characterization of soils by mineral magnetic measurements. *Physics of Earth and Planetary Interiors*, 42, 76-92.
- Maher, B.A., 1988. Magnetic properties of some synthetic sub-micron magnetites. *Geophysical Journal of the Royal Astronomical Society*, 94, 83-96.
- B.A. Maher and R. Thompson, (Eds.), 1999. Quaternary climates, environments and magnetism. Cambridge University Press.
- Oldfield, F. 1991. Environmental magnetism - a personal perspective. *Quaternary Science Reviews*, 10, 73-85.
- Oldfield, F., Brown, A. and Thompson, R. 1979. The effect of microtopography and vegetation on the catchment of airborbe particles, measured by remanent magnetism. *Quaternary Research*, 12, 326 - 332.
- Oldfield, F., Thompson, R. and Dickson, D.P.E. 1981. Artificial enhancement of stream bedload: a hydrological application of superparamagnetism, *Physics of the Earth and Planetary Interiors*, 26, 107-124.
- Oldfield, F., Maher, B.A., Donoghue, J. and Pierce, J. 1985. Particle-size related mineral magnetic source-sediment linkages in the Rhode River catchment, Maryland, U.S.A. *Journal of the Geological Society of London*, 142, 1035-1046.
- Robinson, S.G. 1986. The late Pleistocene palaeoclimatic record of North Atlantic deep-sea sediments revealed by mineral-magnetic measurements. *Physics of Earth and Planetary Interiors*, 42, 22-47.
- Slattery, M.C., Walden, J. & Burt, T.P. 2000. Fingerprinting suspended sediment sources using mineral magnetic measurements: a quantitative approach, in I. Foster (ed.), *Tracers in Geomorphology*, John Wiley & Sons, Chichister, 309-322.
- Thompson, R and Oldfield, F. 1986. *Environmental magnetism*, Allen and Unwin.
- Walden, J. and Addison, K. 1995. Mineral magnetic analysis of a 'weathering' surface within glacial sediments at Glanllynau, North Wales. *Journal of Quaternary Science*, 10, 367-378.
- Walden, J., Smith, J.P. and Dackombe, R.V. 1992. The use of simultaneous R- and Q-mode factor analysis as a tool for assisting interpretation of mineral magnetic data, *Mathematical Geology*, 24, 3, 227-247.

- Walden, J., Dackombe, R.V. and McGraw, J. 1994. Clast lithological and mineral magnetic analysis of diamicts from the Cumberland coastal exposures IN: Boardman, J. and Walden, J. (eds) 1994. *Cumbria Field Guide*, Quaternary Research Association, 15-18
- Walden, J. Smith, J.P. and Dackombe, R.V. 1996. A comparison of mineral magnetic, geochemical and mineralogical techniques for compositional studies of glacial diamicts. *Boreas*, 25, 115-130.
- Walden, J., Slattery, M.C. and Burt, T.P. 1997. Use of mineral magnetic measurements to fingerprint suspended sediment sources: approaches and techniques for data analysis. *Journal of Hydrology*, 202, 353-372.
- Walden, J., Oldfield, F. and Smith, J.P. (eds) 1999. *Environmental magnetism: a practical guide*, Technical Guide Series, No. 6, Quaternary Research Association, London, 250 pp.
- Walling, D.E., Peart, M.R., Oldfield, F. and Thompson, R., 1979. Suspended sediment sources identified by magnetic measurements. *Nature*, 281: 110-113.

A SEDIMENT BUDGET FOR GALVESTON BAY

INTRODUCTION

The Trinity River comprises about 54 percent of the drainage area of Galveston Bay, Texas, and is believed to constitute the major source of sediment to the estuary (Anderson and Rodriguez 2000; Solis et al. 1994; White et al. 2002). Recent studies of sediment flux and storage in the lower Trinity River, however, indicate very low fluvial sediment inputs to the Trinity River delta and Trinity Bay (a portion of Galveston Bay), and extensive alluvial sediment storage upstream of the delta (Phillips et al. 2004). Coastal submergence in excess of the rate of eustatic sea level rise, and land loss in the Trinity River delta system, have been attributed in part to reduced river sediment inputs, which in turn have been attributed to effects of Livingston Dam on the Trinity River (White et al. 2002; Stork and Sneed 2002; Lester and Gonzalez 2002). However, more recent studies have shown that Lake Livingston does not significantly influence sediment dynamics or geomorphic change beyond about 60 km downstream of the dam (Phillips et al. 2004; 2005). Because sediment inputs--fluvial or otherwise--are critical in terms of how Galveston Bay (or other estuaries, particularly on passive margin coastal plains) will respond to sea level rise, better understanding of sediment inputs to the bay is required. While there may be no such thing as a typical or characteristic estuary, even in the restricted setting of the U.S. Gulf Coast, Galveston Bay has at least some broad similarities with other coastal plain estuaries (Nichols 1989), and studies of Galveston Island and Bay have been influential in studies of coastal geomorphic responses to sea level change (Leatherman 1984; Giardino et al. 1995).

The purpose here is to develop an estimated budget of sediment inputs to the Galveston Bay system. There is an emphasis on fluvial sources, but other sources are also considered.

Background

Rivers are not necessarily conveyor belts delivering continental sediment to the sea. This is due to sequestration of sediments in deltas, estuaries, and coastal wetlands, and to alluvial storage upstream of estuaries. Both are relevant to the Galveston Bay problem.

At least for coastal plain rivers on passive margins, this implies that recent trends in river sediment loads discussed by Vörösmarty et al. (2003) and Walling and Fang (2003), however important they may be upstream, may have minimal impact on land-to-ocean sediment fluxes. If upper and lower basins are decoupled in the sense of limited upper-basin sediment being transported to the river mouth, however, then upstream impacts on sediment production and transport (such as dams) may not be evident at the river mouth, however significant the effects upstream. In southeast Texas, for instance, even where large reservoirs controlling 75 to 95 percent of the drainage area of the Sabine and Trinity rivers retain massive amounts of sediment behind dams, no dam-related changes in alluvial sedimentation are noticeable in the lowermost river reaches (Phillips 2003b; Phillips et al. 2004).

Estuaries, deltas, and coastal wetlands may be effective sediment traps. In the U.S. Atlantic drainage, Meade (1982) considers estuaries and marshlands to be the ultimate sink for river sediments, at least on a millennial time scale. He estimates that certainly less than 10 percent, and probably less than 5 percent, of river sediment reaches the continental shelf or deep ocean. Zhang et al. (1990) found that estuarine sinks lead to a similarly small portion of sediment from the Huanghe River reaching the sea. Milliman and Syvitski (1992) note that fluxes to oceans from large rivers (nearly all of which discharge onto passive margins or marginal seas) are overestimated by data from gaging stations due to sediments sequestered in subsiding deltas.

The Pamlico Sound estuarine system, North Carolina, is similar to Galveston Bay in that it is a lagoon with a long water residence time, low capacity-inflow ratio, and low inflow relative to the tidal prism, despite a relatively small tidal range. The Pamlico is an efficient trap for all particulates (Harned et al. 1995; McMahon and Woodside 1997). Though fluvial inputs to the Neuse River estuary (a tributary to the Pamlico Sound) are very low due to extensive storage of coastal plain alluvium (Phillips 1993; 1997), the Neuse is an efficient trap for those particulates that are delivered (Benninger and Wells 1993).

In Texas, while Morton (1994) believes that barrier islands are predominantly made of reworked delta sands, he notes that where rivers discharge into estuaries they do not directly contribute to barrier island sediment budgets. This is broadly consistent with Anderson et al. (1992), who found that southeast Texas barriers are composed of offshore sands, largely derived from drowned deltaic and fluvial deposits of the Trinity and Sabine Rivers.

Multiple studies have shown that some rivers deliver relatively little sediment to the coastal zone, such that sediment delivery to upper estuaries may be severely limited. Ratios of total basin erosion to sediment yield at the outlet of less than 10 percent on an average annual basis has been shown for a number of coastal plain rivers, or upper- and lower-basin decoupling, where so little sediment from the upper basin is transported to the river mouth that they are

essentially decoupled. These include rivers of China (Shi et al. 2003; Zhang et al. 1990), Australia (Brizga and Finlayson 1994; Fryirs and Brierly 1999; 2001; Olive et al. 1994) the south Atlantic U.S. coastal plain (Phillips 1991; 1992a; 1992b; 1993; 1997; Slattery et al. 2002), and Texas Gulf coastal plain (Phillips 2003b; Phillips et al. 2004). The majority of the imbalance between sediment production and sediment yields at the basin mouth is accounted for by source-to-sink time lags, and extensive colluvial and alluvial storage. The well-known relationship between sediment delivery ratios and drainage area, whereby the delivery ratio tends to get smaller as contributing areas increase (Dearing and Jones 2003; Walling 1983), reflects this phenomenon.

Studies of sediment provenance in infilling estuaries with extensive inland drainage basins sometimes show that fluvial inputs are small compared to coastal and marine sediment sources. This is also indicative of extensive alluvial storage in the rivers feeding the estuary. A predominance of coastal sources (such as shoreline erosion) or marine sediment transported landward in such estuaries has been shown for a number of estuaries based on sediment budgets and various tracers or provenance indicators (Marcus and Kearney 1991; Yarbrow et al. 1983; Skrabal 1991; Meade 1969; Hewlett and Birnie 1996; Mulholland and Olsen 1992; Benninger and Wells 1993; Woodroffe et al. 1993).

In summary, previous work on sediment sources in coastal plain rivers and estuaries suggests that Galveston/Trinity Bay may not necessarily be the major sink for fluvial sediments of the Trinity and San Jacinto Rivers, and that fluvial sediment inputs may not be the predominant sediment source to the Bay.

STUDY AREA

Galveston Bay, which includes Trinity Bay (Fig. 1,2) is located in southeast Texas, adjacent to the Houston-Galveston metropolitan area. The estuarine surface area is about 1,554 km², and the total shoreline length about 374 km. Mean volume is estimated at about 2.7 billion m³. The bay is a lagoon-type estuary, separated from the Gulf of Mexico by Galveston Island. The climate is humid subtropical. Using data from the National Estuarine Inventory, Nichols (1989) calculated the ratio between bay volume and mean annual freshwater inflow as 0.2, with a mean water residence time of 40 days. Nichols (1989) also calculated a flow ratio, based on mean freshwater inflow during half a tidal cycle divided by the tidal prism (volume of water exchanged over a tidal cycle) as 0.183.

The bay's drainage area is 85,470 km², of which about 54 percent (46,100 km²) is the Trinity River. The Trinity's headwaters are northwest of the Dallas-Fort Worth area. Lake Livingston, a water supply reservoir, impounds the river about 175 km upstream of Trinity Bay. Most of the drainage area (95 percent) lies upstream of Livingston Dam, which was completed in 1968. Lake Livingston has a conservation pool capacity of more than 2.2 billion m³; its primary purpose is water supply for Houston. The dam has no flood control function and Livingston is basically a flow-through reservoir. Though the lake's capacity is more than 80 percent that of Galveston Bay, analysis of pre- and post-dam discharge records at Romayor found no significant post-dam decrease in flow, and limited change of any kind (Wellmeyer et al. 2005).

The San Jacinto River constitutes about 17 percent of the bay's drainage area (14,504 km²), with the remaining 29 percent (24,866 km²) accounted for by various smaller coastal watersheds.

The coast around Galveston Bay is experiencing erosion along barrier beaches and subsidence and wetland loss in its estuaries. Along Galveston Island 57 percent of the shoreline has experienced erosion rates averaging 0.6 m/yr or more in recent years, while on Bolivar Peninsula the figure is 86 percent. In the Galveston Bay estuarine system, which includes the Trinity Bay and Trinity River delta, shoreline retreat of 1.5 to >3 m yr is common in recent years, and conversion of marshes to open water at a rate of 47 ha/yr has been documented for the Trinity Delta (Morton and Paine 1990; White and Calnan 1991; Morton 1993; GLO 2001). The erosion and land loss has, in many cases, accelerated within the past 50 years. White and others (2002) note that the Trinity River Delta was prograding through most of the 20th century, with a transition to degradation beginning between 1956 and 1974. Beach erosion in Texas shows an apparent increase beginning in the 1960s (Davis 1997; Morton 1977, Morton and Paine 1990). The increase in erosion and land loss roughly coincides with the impoundment of the Trinity and other Texas rivers and suggests the possibility that, in addition to the other factors that influence coastal geomorphology, human modifications of both coastal systems and the fluvial systems draining to them may be contributing to erosion and coastal land loss.

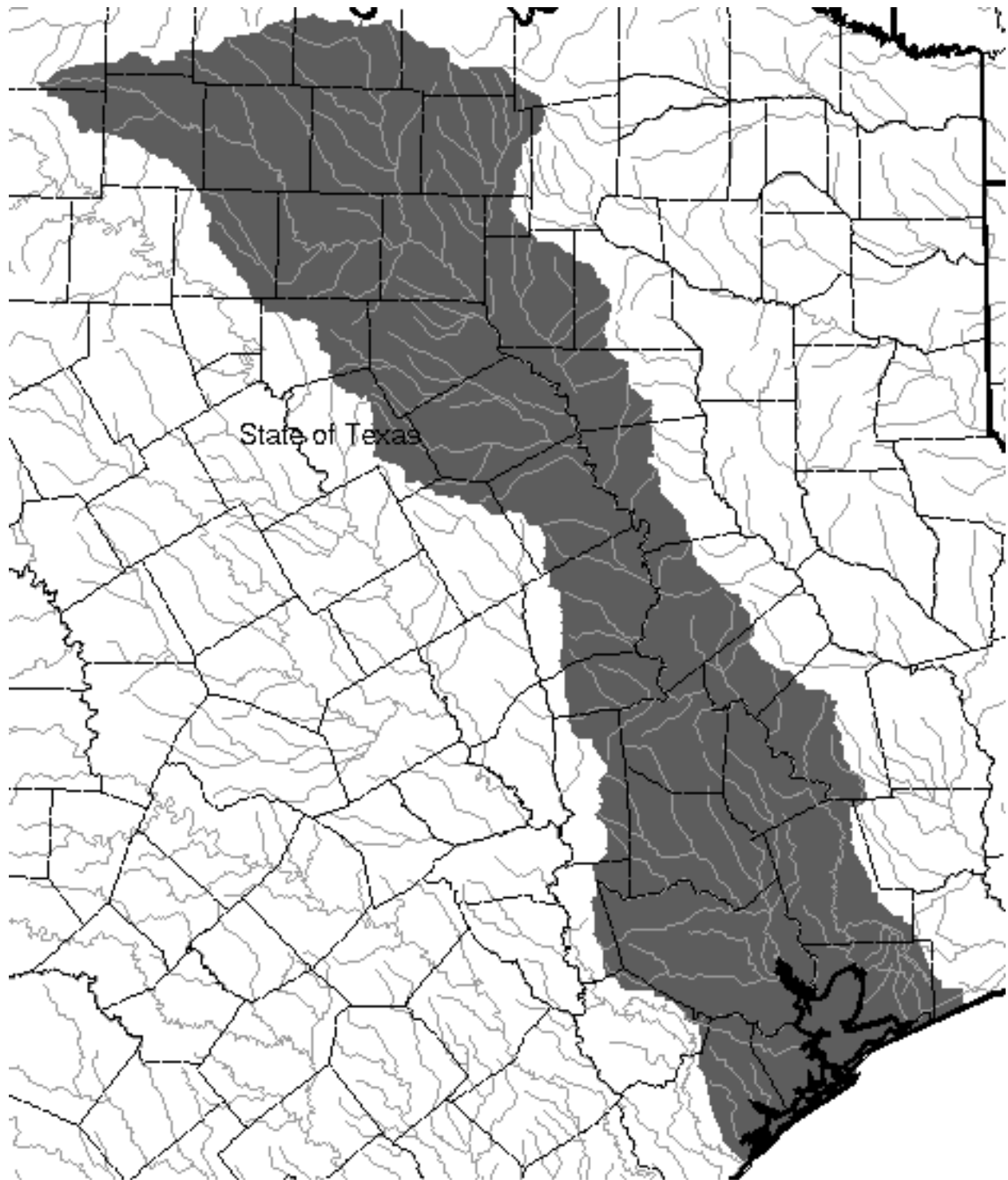


Figure 1. Galveston Bay watershed (shaded). County outlines and major streams also shown. Adapted from U.S. Environmental Protection Agency map available at <http://www.epa.gov/owow/estuaries/programs/sheds/gb.gif>. Scale is approximately 1:3,142,125.



Figure 2. Galveston Bay area, derived from MODIS satellite image acquired Nov. 6, 2002. Numbered items are (1) Galveston Bay; (2) Trinity Bay; (3) Bolivar Roads inlet; (4) central Houston, Texas; (5) Lake Livingston.

However, in the Trinity River and some other east Texas streams sediment starvation effects of dams are concentrated in a limited zone downstream of the dam, and may be unnoticeable in the lower reaches (Phillips 2001; 2003; Phillips and Marion 2001; Phillips and Musselman 2003; Phillips et al. 2004; 2005). This is due in part to replenishment of sediment loads by tributary inputs and lower-basin erosion, and by channel erosion in a scour zone downstream of the dam, the latter being particularly important in the Trinity (Phillips et al. 2004). More fundamentally, however, there are often sediment transport bottlenecks in lower reaches of coastal plain alluvial rivers, where ample accommodation space and low stream power reduce sediment transport capacity and promote alluvial storage. This means that the locus of alluvial deposition is upstream of bayhead deltas and estuaries, and that transport of river sediment to the estuary would be low with or without dams upstream. In the lower Trinity River downstream of Romayor, accommodation space increases somewhat, the frequency of overbank flow increases, and slope and stream power (and thus transport capacity) decline dramatically. Additionally, the channel bed is cut to below sea level, and the river is subject to coastal backwater effects, and channel morphological responses to sea level rise extend about 115 km above Trinity Bay (Phillips et al 2004; 2005; Phillips and Slattery 2005).

The wetland loss in the Galveston Bay area has been well-documented, and White et al. (2002) used ^{210}Pb methods to examine marsh sedimentation trends in the Trinity and two other Texas fluvial-deltaic systems. Long-term average sedimentation rates for the Trinity delta were $5.14 \pm 0.00008 \text{ mm yr}^{-1}$. Rates for the 12 individual cores ranged from 1.6 to 13 mm yr^{-1} . White and Calnan's (1991) historical analysis shows that the delta prograded from 1930 to 1956, after which marsh conversion to open water began dominating in the 1956 - 1974 time interval.

The alluvial morphology and stratigraphy of the lower Trinity (and the nearby and similar Sabine River), and the deposits and paleochannels now submerged in Trinity and Galveston Bays and the Gulf of Mexico preserve evidence of climate, sea level, and upstream sediment delivery changes (Anderson and Rodriguez 2000; Anderson et al. 1992; Blum et al. 1995; Phillips 2003; Phillips and Musselman 2003; Rodriguez and Anderson 2000; Rodriguez et al. 2001; Thomas and Anderson 1994). Therefore contemporary modifications to flow and sediment regimes are superimposed on long term changes controlled primarily by climate and sea level change.

The details of sea-level history and coastal evolution in Texas are controversial (Blum et al. 2002), but all sources agree that Galveston Bay was formed about 4000 years ago. During lower Quaternary sea level stands, the Trinity and Sabine Rivers converged on the continental shelf and cut an incised valley. From about 18,000 years BP to the present, the Trinity-Sabine incised valley has backfilled. During this transgression the Brazos, Colorado, and Rio Grande rivers filled their incised valleys and prograded delta plains, presumably due to higher sediment yields than the Trinity, Sabine, Guadalupe, and Nueces rivers, which discharge to bayhead deltas and drowned-valley estuaries fronted by barrier islands (Blum et al. 1995; 2002).

SEDIMENTATION IN GALVESTON BAY

Contemporary sediment accumulation rates in Galveston Bay are difficult to determine, due to disturbance of the bay bed associated with dredging, navigation, oyster harvesting, and hydrocarbon exploration and production. Recent and historical rates estimated from bathymetric surveys compared to historical maps indicate mean sediment accumulation rates of 3.5 mm yr⁻¹, while longer-term Holocene rates based on radiocarbon dates and isopach charts of Holocene fill suggest a mean rate of 3.8 mm yr⁻¹ (Nichols 1989; Shepard 1953).

Based on typical bulk densities of estuarine and lake sediments and freshly-deposited alluvium, it is common to assume a density of about 1 tonne m⁻³ (Smith et al. 2002; Phillips et al., 2004). Based on this, mean sedimentation rates of 3.5 to 3.8 mm yr⁻¹ over the area of the bay would require 5,439,000 to 5,905,200 t yr⁻¹ of sediment input.

The amount of sediment input required to keep pace with sea level rise makes a convenient reference point, though in fact estuaries are geologically ephemeral, and there is no reason, based on geomorphological principles or on the Quaternary history of the southeast Texas coast, to expect Galveston Bay to maintain its area or volume in response to sea level change.

Leatherman's (1984) analysis of potential Galveston Bay shoreline erosion responses to sea level rise used a baseline scenario for 1980 - 2075 period of 3.2 mm yr⁻¹. Nichols (1989) reported short-term rates of 5.5 mm yr⁻¹ from tidal gage records and long-term rates of 1.4 mm yr⁻¹. Coastal submergence (accounting for sea level change and land surface elevation changes) is substantially higher, averaging about 7.6 mm yr⁻¹ from recent tidal gage records and interferometry measurements (Stork and Sneed 2002). White et al. (2002) combine an estimated eustatic sea level rise of 2.2 mm yr⁻¹ with mean subsidence of 8.1 mm yr⁻¹ at four lower Trinity valley benchmarks to arrive at an estimate of 10.3 mm yr⁻¹ relative sea level rise (coastal submergence).

Using the same assumptions as above, mean annual sediment inputs of just under 5 million tonnes would be necessary to offset an annual sea level rise of 3.2 mm, and about 11.8 million for coastal submergence of 7.6 mm yr⁻¹.

Sediment inputs

There are three general potential sources of sediment to Galveston Bay. These are fluvial input, including local runoff around the bay margins, coastal and marine sources derived from barrier island overwash or transported through Bolivar Roads, and shoreline erosion. Aeolian input is also possible, but is likely to be negligible compared to other inputs. Maximum dust deposition on tank trails at Fort Hood Texas was measured at a rate amounting to 2.3 X 10⁻⁵ mm yr⁻¹, calculated from data in Gebhart et al. (1996). As dust deposition rates in the Galveston Bay area are likely to be a minuscule fraction of those on highly-disturbed dry dirt trails, the aeolian contribution can be discounted. While landward wind transport of beach and dune sands may be locally significant in the backbarrier areas, we consider this as part of the coastal input.

In addition to sediments newly supplied to the Trinity delta and Galveston Bay, reworking within the bay and delta locally transfers sediment within the system.

Trinity River sediment inputs have historically been estimated based on measurements at the U.S. Geological Survey gaging station at Romayor, about 123 km upstream of Trinity Bay. U.S. Geological Survey and Texas Water Development Board records going back to 1936 show a clear decline in sediment loads at Romayor following

completion of Livingston Dam in 1968, about 52 km upstream of Romayor (White and Calnan 1991; Solis et al 1994; Wellmeyer et al. 2005; Phillips et al. 2005). However, daily suspended sediment samples were taken from 1965-1989 at a gaging station at Liberty, Texas, further downstream. These records not only show sediment transport far lower than even the post-dam rates at Romayor, but also indicate no discernible effects of Livingston dam (Phillips et al. 2004). The Liberty data provide the basis for the best estimate of actual delivery of sediment by the Trinity River to its delta and the bay, though even this station undoubtedly overestimates fluvial input (Phillips et al. 2004). There are no comparable data for the San Jacinto and other coastal watersheds draining to Galveston Bay.

METHODS

Fluvial sediment inputs

The Texas Water Development Board (TWDB) collected daily suspended sediment samples at three stations on the Trinity River (Liberty and Romayor downstream and Crockett upstream of Lake Livingston) and Long King Creek over the 1964-1989 period. All sampling locations are U.S. Geological Survey gaging stations, and the measured concentrations were converted to daily transport values based on the mean daily flows recorded at the gaging stations. The samples were taken with the "Texas Sampler," a point-sampler which yields results lower than, but systematically related to, yields based on depth-integrated sampling using standard U.S. Geological Survey methods (Andrews 1982; Welborn 1967). Values at the Romayor station were compared to same-day samples collected by the USGS, indicating that a multiplier of 2.37 should be used to convert TWDB values to equivalent depth-integrated values. Similar results were obtained in comparing the Texas sampler to U.S.G.S. depth-integrated samples by Andrews (1982) and Welborn (1967).

The suspended sediment measurements underestimate transport by not accounting for bedload. It is customary in many studies to add 10 percent to account for bedload. At the Romayor station on the Trinity River, on 12 occasions in 1972-1975 the U.S. Geological Survey measured suspended and bed load on the same day. Bed load represented 1.4 to 21.4 percent of total sediment load, with a mean of 9.7 percent. Thus sediment transport estimates based on suspended measurements alone were increased by 10 percent.

While the Liberty records are the closest estimate of Trinity River sediment outflux to the estuary, the Long King Creek records might reasonably be used as an indicator of sediment production from the lower basin. The Long King Creek station at Livingston, Texas, has a drainage area of 365 km² and is an unregulated tributary of the Trinity.

Independent estimates of sediment delivery to streams in the lower Trinity basin are available from reservoir surveys conducted by the Texas Water Development Board. The surveys document changes in reservoir capacity. If these are assumed to be due to sedimentation, dividing the capacity change by the number of years between surveys gives a volume of sediment accumulation per year. This is further adjusted for drainage areas to produce a virtual rate in m³ km⁻² yr⁻¹. Bulk density of newly-deposited lake sediments in Texas range from 0.5 to 0.9 Mg m⁻³, and those of older, more compacted lake sediments are typically 1.1 to 1.3 (Welborn 1967; Williams 1991). Thus, we again assume a density of 1 Mg m⁻³, a conservative estimate which follows the practice of Smith et al. (2002). Data for 27 lakes in east and central Texas were examined by Phillips et al. (2004). For this study, the focus is on data for two lakes within the coastal plain portion of the Galveston Bay drainage area (Lakes Houston and Conroe), and for Lake Steinhagen, a coastal plain reservoir in the Neches River system which was not included in previous work.

The amount of sediment in the Trinity River bayhead delta was estimated by measuring the total surface area from maps, and determining mean thickness from facies maps prepared by McEwen (1963).

Shoreline erosion is a significant sediment source in many estuaries, and Galveston Bay shorelines are no exception. Rates of shoreline retreat have been measured based on comparisons of aerial photographs (Morton and Paine 1990; White and Calnan 1991; Morton 1993; GLO 2001). While shoreline erosion rates are invariably episodic, Hall et al. (1986) found that short-term rates for a portion of the bay shore over a period including several storms did not differ appreciably from the longer-term rates derived from aerial photographs. To convert shoreline retreat to mass or volume estimates of sediment, the vertical dimension must be known. About 61 percent of the bay shore is marshes or other wetlands (Lester and Gonzalez 2002), and even where bluff shorelines exist, there is typically a small beach at the bluff toe. The relief of intertidal marsh shores or beach scarps is typically the same order of magnitude as the tidal range, which is 0.2 to 0.3 m. Thus sediment contributions from shoreline erosion per unit of shoreline length are estimated by multiplying the retreat rate (m yr⁻¹) by 0.3.

To qualitatively assess the relative importance of newly-delivered river sediment versus reworking, 34 sediment samples were collected from the Trinity River delta. Samples were immediately sealed in polyethylene containers for transport to the laboratory. The Munsell color was recorded in the wet or moist condition immediately on

exposure. Munsell color was recorded under identical light conditions exactly 24 and 48 hours after exposure, with moisture added with an eyedropper where samples had dried beyond moist conditions. All samples were fully air-dry within 48 hours. The color of fine-grained alluvium, and reoxidation of reduced samples elsewhere in east Texas was shown by Phillips and Marion (2001) to provide an indicator of redox status and in certain circumstances, residence time.

The sand fraction was examined under a binocular microscope with special attention to texture, oxide and other grain coatings, the rounding or angularity of sand grains, and color. The primary purpose was an attempt to determine the extent to which alluvial deposits represent “new” sediment from uplands in the lower Sabine basin as opposed to reworked deltaic material.

Grain angularity was classified as angular if there were non-rounded corners and sharp edges or protuberances. Where edges and irregularities were evident but rounded, the grains were classified as subangular. Grains with no major edges or irregularities but with some etching and pitting were classified as subrounded, and rounded grains were entirely smooth.

Coatings of Fe oxides on sand grains (any brown, yellow, red, or orange coating was assumed to be Fe oxides) were assessed on a categorical scale, whereby the terms many, common, few, rare, or none were applied when the number of coated sand grains observed under the microscope was, respectively, >50, 10 to 50, 1 to 10, or <1 percent, or completely absent.

More detailed and sophisticated assessments of the lithology, geochemistry, and weathering of fluvial sands have been used to shed light on the sources of sand and weathering during alluvial storage (Johnsson and Meade, 1990; Johnsson et al., 1991; Stallard et al., 1991). However, less expensive methods similar to those employed here have been used in other studies, and are useful in as general indicators. The degree of rounding or angularity of grains is related to abrasion during transport, and can provide an indication of the time or distance of transport. Roundness increases (and angularity decreases) systematically downstream (Mills, 1979; Knighton, 1998: 136-140). Stanley et al., (2000) showed that iron-staining of sand grains could be used to distinguish *in situ* Pleistocene deltaic sediments from reworked Holocene material. This suggests that the length or intensity of reworking results in the loss of iron stainings and coatings. Eriksson et al., (2000) used intact iron oxide coatings of sand grains in colluvial and alluvial deposits as an indicator transport has occurred over relatively short distances.

RESULTS

Fluvial sediment delivery

The gaging station on Long King Creek at Livingston has a drainage area of 365 km², and a mean annual sediment yield of 467 t km² yr⁻¹. As shown in Table 1, this is considerably higher than sediment yield per unit area for any of the stations on the lower Trinity River, including the Crockett station upstream of Lake Livingston. At Liberty, where the gage datum is 0.7 m below sea level, the specific sediment yield is less than 1.6 t km² yr⁻¹. The inverse relationship between drainage area and sediment yield per unit area evident in Table 1 is consistent with many other studies in humid perennial streams where the major source of sediment is upland erosion and tributary inputs within the basin (this literature is reviewed by Ferro and Minacapilla 1995; Meade 1982; Sutherland and Bryan 1991; and Walling 1983). Recall that sediment yield at the Romayor station has been reduced by Lake Livingston.

The lake surveys suggest sediment yields of 6 to 578 t km² yr⁻¹. The two lakes in the bay drainage and close to the bay, Houston and Conroe, give results two orders of magnitude different. It is possible that capacity changes may be due to factors other than sedimentation, such as dredging, shoreline erosion or modifications, flushing flows, or dam modifications. Part of the difference may be accounted for by drainage area, as sediment yield per unit area typically declines with drainage area, and Lake Houston has a drainage area more than six times that of Lake Conroe. As Lake Houston is downstream of Lake Conroe, it is also possible that sediment inputs are reduced by trapping within the upstream lake. With respect to Lake Conroe, the lake survey report specifically attributes the volume reduction to sedimentation (Sullivan et al. 2003). While the Lake Houston sediment yields are low compared to those estimated from other reservoir surveys, there is corroborating evidence. Van Metre and Sneck-Fahrer (2002) took sediment cores from Lake Houston in 1997 to examine trends in water quality. One core was analyzed for ¹³⁷Cs data, which showed about 105 cm of sedimentation since reservoir construction in 1954, with relatively constant rates of accumulation. This core, if extrapolated over the entire lake with an assumed density of 1 g cm⁻³, implies a sediment yield of 3.7 t km² yr⁻¹, which suggests that the yield estimated from the capacity survey is not too low.

Table 1. Fluvial sediment yields in the Galveston Bay region.

Source of Measurement/Estimate	Drainage Area km ²	Yield, t km ⁻¹ yr ⁻¹
Long King Creek at Livingston (1)	365	467
Trinity River at Crockett (1)	36,029	142
Trinity River at Romayor (1)	44,512	76
Trinity River at Liberty (1)	45,242	1.6
Trinity River at Trinity Bay (2)	46,100	<1.6
Houston Lake (3)	7,325	6
Lake Conroe (4)	1,153	189
B.A. Steinhagen Lake (5)	19,614	50.2

(1) Based on 1964-1989 sediment sampling by the Texas Water Development Board, adjusted as described in text, and previously reported by Phillips et al. (2004).

(2) Estimated by Phillips et al. (2004)

(3) Based on reservoir capacity loss, from Texas Water Development Board reservoir surveys. Source: <http://www.twdb.state.tx.us/assistance/lakesurveys/surveytech.htm>.

(4) Source: calculated from data in Sullivan et al. (2003).

(5) Source: calculated from data in Austin et al. (2004).

The yields reported in Table 1 can be compared with other studies in the region (Table 2), which focusses mainly on relatively small drainage areas or estimates which might be applied to estimate local sediment yields in the coastal watersheds surrounding Galveston Bay. Per-unit-area sediment yield for large drainage areas would be much lower (see Table 1).

Table 2. Fluvial sediment yields in the east Texas coastal plain.

Location	Yield	Source (t km ⁻² yr ⁻¹)
Lower Trinity River Basin	400	Phillips et al. 2004
Lower Trinity River Basin	36	Greiner 1982
Mean for 27 E. Texas reservoirs	375	Phillips et al. 2004
Steinhagen Lake	50	This study; Austin et al. 2004
Lake Houston	6	This study; Phillips et al. 2004
Lake Conroe	189	This study; Sullivan et al. 2003
Angelina River basin, forested	3.3	Blackburn et al. 1986
Angelina River basin, logged	19 to 294	Blackburn et al. 1986
Angelina National Forest	2 to 70	Blackburn et al. 1990
Buffalo Bayou & lower San Jacinto	143	Greiner 1982

In estimating sediment inputs to Galveston Bay, 70,000 t yr⁻¹ (slightly higher than the measured mean annual load at Liberty) is a reasonable figure for the Trinity River. For the remaining 46 percent of the Galveston Bay watershed, contained entirely within the coastal and coastal plain regions, mean annual yields of 6 to 190 t km⁻² yr⁻¹ might reasonably be applied, producing lower and upper bounds of 236,220 and 7,480,300 t yr⁻¹. Our “best professional judgement” estimate is about 60 t km⁻² yr⁻¹, producing (with the Trinity contribution) 2,432,200 t yr⁻¹. These estimates are summarized in Table 3.

Table 3. Sediment Inputs to Galveston Bay (see text for explanation).

<i>Source</i>	t yr^{-1}
Fluvial	
Trinity River	70,000
Other	
Minimum	236,220
Most likely	2,362,200
Maximum	7,480,300
Shoreline erosion	81,800
Total	388,020 to 7,632,100

Trinity River Delta

The surface area of the delta, excluding large open-water areas, is 126.1 km². Facies maps of McEwen (1963) indicate a mean thickness of about 3.1 m, implying a total sediment volume of 390,910,000 m³. Assuming delta accumulation began 4000 Ka, this indicates a mean accumulation rate of 97,727 t yr⁻¹.

Shoreline erosion

Mean historical shoreline retreat rates are 0.73 m yr⁻¹ (Morton and Paine 1990; White and Calnan 1991; Morton 1993; GLO 2001), averaged over the 374 km of shoreline. Assuming 0.3 m relief, this would produce 81,800 tonnes per year.

Sediment characteristics

Color. Sediment eroded from slopes within the basin, and from most river banks, will not exhibit colors indicative of gleying (Munsell chroma < 3) unless it has been stored in a reducing environment long enough for iron to be reduced. The longer such sediment resides in subaqueous or saturated settings, the more the ferrous, soluble iron is lost. Gleyed sediments which have not been stored long enough for all iron to be lost will change color upon exposure to air, showing increases in Munsell value and/or chroma and/or shifts to redder hues as remaining iron is oxidized. The principles associated with relating color and color changes to residence time are discussed in more detail by Phillips and Marion (2001) and references therein.

The Trinity River Delta samples, with five exceptions, had colors indicating a predominantly reduced, gleyed condition (Table 4). These five exceptions included two with chromas of 3, and three sandy samples where the color was dominated by light-colored sand. Even in the latter cases, finer material had Munsell chromas ≤ 2 . The higher chroma samples were from sites on Old River and Turtle Bayou where pre-Holocene terraces are being eroded, and where samples were collected to confirm the color/redox status of potential sediment sources within the delta which are not in reducing environments. Color changes of a single unit of Munsell hue, value, or chroma could readily be attributed to operator variance, but in 18 cases color changes on exposure amounted to two or more units of hue, value, or chroma, or changes of at least one unit in two or more of hue, value, and chroma. However, in 16 of the 18 cases these color changes were insufficient to move the color designation from the gleyed range.

In general, these samples did not have substantial amounts of remaining iron, and the observed color changes may be attributed to oxidation of trace amounts of Fe and other substances, changes in moisture content (though colors were always measured on moistened surfaces), and operator variance.

Angularity and Coatings. None of the 34 sediment samples had dominantly angular sand grains. In 12 cases there was insufficient sand to make a reliable determination of coatings or angularity. Eight samples had dominantly subangular, 12 subrounded, and two rounded grains. Only one sample had “many” Fe oxide-coated grains. Five were in the common, 11 in the few, three in the rare, and two in the none categories.

SEDIMENT BUDGET

The best estimate of fluvial and shoreline erosion inputs imply a sediment deficit relative to bay sedimentation rates of nearly 3 million tonnes per year (Table 5). Assuming reasonable accuracy with respect to Galveston Bay infill rates, the deficit may be attributable to one or all of the following: aeolian input, underestimation of fluvial input, and sediment from coastal sources other than bay shoreline erosion. These will be addressed in the discussion.

Table 6 shows the relative contributions of water and sediment for the Trinity River and the remainder of the Bay drainage basin. The proportion of total sediment input (Bay infill) reflects the deficit described above. The proportion of total water inflow is based on the flow ratio (freshwater inflow relative to tidal prism) of 0.183. The table shows that while the Trinity represents 54 percent of the drainage area and freshwater inflow, it contributes substantially smaller proportions of sediment. This is undoubtedly in part due to the fact that 95 percent of the Trinity River drainage basin is more than 175 river km upstream of the Bay, and that the locus of deposition in the lower Trinity is upstream of the delta (Phillips et al. 2004).

Table 4. Color (Munsell notation), angularity, and coatings for delta sediment samples. Colors are given for initial (field) conditions, and after 48 hours dry exposure. Where no angularity or coatings data are given there was insufficient sand to make assessments.

Sample		Color		Angularity	Coatings
		initial	48 hr		
1	bank	gley1 2.5/N	gley1 4/N		
2	bank	2.5Y 5/2	2.5Y 5/2	subrounded	common
3	CM ¹	sand ²	sand	rounded	none
4	PB ³	sand	sand	rounded	none
5	floodplain	5Y 4/1	2.5Y 4/1		
6	CM	5Y 4/1	2.5Y 6/2	subangular	few
7	floodplain	10YR 4/1	2.5YR 5/2		
8	bank	2.5Y 4/2	2.5Y 5/2		
9	CM	5Y 4/1	10YR 7/2	subrounded	few
10	floodplain				
11	CM	5Y 4/1	2.5Y 5/2		
12	CM				
13	floodplain	2.5Y 5/2	2.5Y 6/3	subangular	few
14	marsh	10YR 4/2	10YR 5/2	subrounded	few
15	marsh	10YR 3/1	10YR 4/1		
16	CM	2.5Y 4/3	2.5Y 5/2	subangular	rare
17	PB	sand	sand	subrounded	few
18	marsh	2.5Y 3/1	2.5Y 5/2	subrounded	many
19	CM	2.5Y 4/1	2.5Y 6/2	subrounded	common
20	marsh	5Y 4/1	2.5Y 5/2	subangular	few
21	mudflat	5Y 5/1	2.5Y 6/2	subrounded	few
22	CM	Gley1 4/N	2.5Y 7/2		
23	floodplain	2.5Y 5/1	2.5Y 5/2		
24	CM	5Y 4/1	2.5Y 6/2	subangular	few
25	channel	gley1 3/N	2.5Y 6/2	subangular	rare
26A	channel	gley1 4/N	2.5Y 6/2		
26B	channel	5Y 3/1	2.5Y 4/1		
27	floodplain	2.5Y 4/1	2.5Y 5/2	subangular	few
28	bank ⁴	2.5Y 5/4	2.5Y 6/4	subrounded	common
29	marsh	2.5Y 4/1	2.5Y 3/1		
30	floodplain	2.5Y 4/2	2.5Y 6/3		
31	CM	5Y 4/1	2.5Y 6/2	subrounded	few
32	marsh	gley1 3/N	gley1 3/N		
33	marsh	2.5Y 4/1	2.5Y 4/1	subrounded	common
34	CM	5Y 5/1	2.5Y 5/2	subrounded	common
35	bank ⁴	2.5Y 5/3	2.5Y 6/4	subrounded	few

¹channel margin; ²denotes sample with $\geq 90\%$ sand; ³point bar; ⁴eroding Pleistocene terrace

Table 5. Galveston Bay sediment budget ($t\ km^{-2}\ yr^{-1}$). See text for explanation of estimates. Note that the deficit rows reflect the minimum, maximum and best estimate sediment deficits (for example the maximum input minus the minimum sedimentation rate gives the minimum deficit relative to infill).

	Minimum	Maximum	Best Estimate
Bay Sedimentation	5,439,000	5,905,200	5,500,500
Rate to keep pace with sea level	5,000,000	11,800,000	5,000,000
Input	388,020	7,632,100	2,514,000
Deficit relative to infill	none (surplus)	5,517,180	2,986,000
Deficit relative to sea level	none (surplus)	11,411,980	2,486,000

Table 6. Relative contributions of water and sediment for the Trinity River and remainder of the Galveston Bay watershed.

Percentage of:	Trinity River	San Jacinto & coastal basins
Drainage area	54	46
Freshwater inflow	54	46
Total water inflow	10	8
Fluvial sediment input	2.9 (0.9 to 23)	97.1 (77 to 99.1)
Total sediment input	1.3	45.7 (5.4 to 45)

Sources: GBFIG 2003; this study.

DISCUSSION

The Trinity River basin comprises the majority of the drainage area for Galveston Bay, and contributes more than half the average freshwater inflow. Relatively little Trinity River sediment is delivered to Galveston Bay, however. This is not particularly surprising, as previous work has shown extensive alluvial storage upstream of the Trinity bayhead delta, and low sediment transport capacity in the lower Trinity (Phillips et al. 2004; 2005). The locus of deposition is upstream of the estuary, accounting for the low input of river sediment to Trinity and Galveston Bays.

The remaining 46 percent of the Bay watershed provides the majority of the fluvial sediment. The greater sediment yield per unit area as compared to the Trinity River basin is due to closer proximity to the estuary, leading to shorter transport distances and lag times, and fewer alluvial storage opportunities.

Unless fluvial erosion in the coastal watersheds surrounding the Bay is substantially higher than the data suggest, fluvial sediment cannot begin to account for observed sedimentation in Galveston Bay or to provide enough sediment to keep pace with sea level rise. This may be attributable to one or all of the following: aeolian input, underestimation of fluvial input, and sediment from coastal sources.

As discussed earlier, aeolian input is not likely to be a significant contributor to infilling. As indicated in Table 5, while the best estimate and some alternative scenarios result in a sediment deficit, other scenarios eliminate the

deficit or even create a surplus (e.g., sediment influx to the bay greater than the bay infill rate). We do not believe the fluvial inputs are underestimated, for several reasons. First, the Trinity River estimate (mean input of 70,000 t yr⁻¹) is based on about 25 years of daily measurements at Liberty. This is corroborated by the apparent average long-term sediment accumulation rate in the bayhead delta of about 98,000 t yr⁻¹, as it is reasonable to assume that higher rates of accumulation occurred in the early stages of delta development that would more closely resemble input rates that now exist in the Trinity River reach upstream of Liberty. Additionally, the contemporary and historical sediment transport, alluvial sediment storage, and geomorphic responses of the lower Trinity upstream of the delta are well documented (Phillips et al. 2004; 2005; Wellmeyer et al. 2005). Second, the estimated mean annual input of 60 t km⁻² yr⁻¹ for the non-Trinity portion of the Galveston Bay watershed is probably too high for the San Jacinto portion of the basin, based on sediment accumulation rates in Lake Houston.

Coastal sediment inputs have not been accounted for other than erosion of the Bay shoreline. While we believe this estimate is reasonable and are confident in the recession rates used, assuming a vertical dimension of greater than the 0.3 m we used here would generate more sediment. Overwash and aeolian sediments from Bolivar Peninsula and Galveston Island are other possible sources, but are likely to be minor, particularly since construction of the Galveston seawall nearly a century ago. The other major sediment source is transport into the Bay through Bolivar Roads inlet. Satellite imagery shows sediment plumes both into and out of Galveston Bay through the inlet, depending on tides and wind. Bolivar Roads has both flood- and ebb-tidal deltas, and Rodriguez et al. (1998) found that the flood and ebb deltas are of comparable size, and that such deltas have been maintained throughout Holocene sea level transgression. A significant portion of the incoming sediment transported beyond the flood-tidal delta (presumably mostly fine-grained material) is likely to remain within the Bay. The fact that the tidal prism greatly exceeds typical freshwater inflows also supports the importance of coastal/marine sources to Galveston Bay. The relative contribution of various sediment sources is shown graphically in figure 3, using the best estimate figures from table 5.

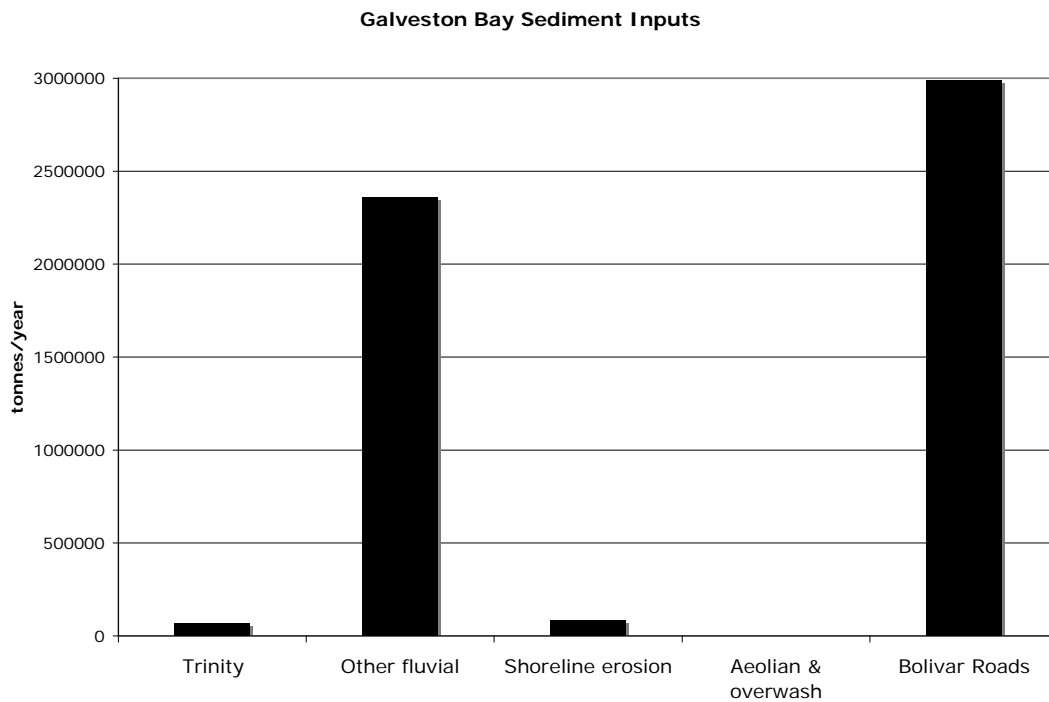


Figure 3. Relative sediment contributions to Galveston Bay, on an average annual basis.

The Trinity River delta is undergoing a net loss of land and conversion of marsh to open water. Coastal submergence rates which account for subsidence as well as sea level rise exceed sedimentation rates. This is consistent with the notion that the modern delta is largely composed of reworked or earlier Holocene material. Color, angularity, and grain coatings of delta sediment samples suggest relatively long (> 1 year) residence times, and little or no sediment recently eroded from uplands. While subrounded and rounded grains could have been eroded from Pleistocene alluvial terrace deposits (as reductions in angularity are irreversible), terrace soils are generally Fe oxide-coated.

The combination of Bay shoreline erosion, land loss in the Trinity River delta and other wetlands, and coastal submergence (relative sea level rise) indicate a short-term enlargement of Galveston Bay. None of these are

attributable to recent, human-caused reduction of sediment inputs from the Trinity River, though the upstream migration of the locus of deposition in the river during Holocene sea level rise no doubt plays a role. Human activity may have reduced sediment inputs from the San Jacinto River due to sediment storage in Lakes Houston and Conroe, but these effects (like those of Lake Livingston) may be localized immediately downstream of the dams. In any case, they are likely at least partly offset by increases in erosion associated with urbanization, agriculture, and forestry in the densely-populated Bay region.

It would not be wise to extrapolate current trends more than a few years into the future. The Holocene and Quaternary evolution of the Galveston Bay system has been characterized by episodic, sometimes abrupt changes in forcings (e.g. sea level) and responses. More recently, the lower Trinity River and Trinity Delta have experienced qualitative changes in geomorphic responses.

CONCLUSIONS

General conclusions are:

- The Trinity River, while accounting for a majority of the drainage area and freshwater inflow to Galveston Bay, delivers only a small amount of sediment, about $70,000 \text{ t km}^{-2} \text{ yr}^{-1}$ on average.
- Sediment inputs from the remainder of the watershed may be as low from 6 to $190 \text{ t km}^{-2} \text{ yr}^{-1}$. At the average rate of $60 \text{ t km}^{-2} \text{ yr}^{-1}$, this would provide a mean of $2,360,200 \text{ t km}^{-2} \text{ yr}^{-1}$.
- Fluvial sediment inputs are insufficient to account for observed sediment infill rates in Galveston Bay, or to keep pace with eustatic sea level rise.
- Erosion of the bay shoreline is a significant sediment source. The estimated mean contribution is $81,800 \text{ t yr}^{-1}$, but this could be higher.
- The other likely major sediment source to the Bay is transport of Gulf of Mexico sediments through Bolivar Roads inlet.
- About 126,100,00 tonnes of sediment are stored in the Trinity River delta, indicating mean accumulation rate of $97,727 \text{ t yr}^{-1}$ over 4000 years.
- Delta sediments have color, angularity, and Fe oxide coatings indicative of a relatively long fluvial residence time, with limited input of recently-eroded upland sediments.
- Galveston Bay is enlarging due to shoreline erosion, conversion of wetlands to open water, and net coastal submergence. Human-caused reductions in fluvial sediment input are a minor contributor to this trend, if they are significant at all. Other human activities, however, such as hydrocarbon and groundwater extraction (which contribute to subsidence) may play a role.

REFERENCES

- Anderson, J.B., Rodriguez, A.B., 2000. Contrasting styles of sediment delivery to the east Texas shelf and slope during the last glacial-eustatic cycle: implications for shelf-upper slope reservoir formation. *Gulf Coast Association of Geological Societies Transactions* 50, 343-347.
- Austin, B., Thomas, D., Burns, R., Sansom, M. 2004. Volumetric Survey of B.A. Steinhagen Lake. Austin: Texas Water Development Board, 42 p.
- Anderson, J.B., Thomas, M.A., Siringan, F.P., Smyth, W.C. , 1992. Quaternary evolution of the east Texas coast and continental shelf. In C.H. Fletcher III and J.F. Wehmiller, eds., *Quaternary Coastlines of the United States: Marine and Lacustrine Systems*, SEPM (Society for Sedimentary Geology), 253-263.
- Andrews, F.L., 1989. Monthly and annual suspended sediment loads in the Brazos River at Richmond, Texas, 1966-1986 water years. U.S. Geological Survey, Department of the Interior. Water Resource Investigation Report 88-4216.
- Blum, M.D., Morton, R.A., Durbin, J.M., 1995. "Deweyville" terraces and deposits of the Texas Gulf coastal plain. *Gulf Coast Association of Geological Societies Transactions* 45, 53-60.
- Blum, M.D., Price, D.M. , 1994. Glacio-Eustatic and Climatic Controls on Quaternary Alluvial Plain Deposition, Texas Coastal Plain. *Gulf Coast Association of Geological Societies Transactions* 44, 85-92.
- Davis, R.A. 1997. Regional coastal morphodynamics along the U.S. Gulf of Mexico. *Journal of Coastal Research* 13, 595-604.
- Gebhart, D.L., Hale, T.A., Michaels-Bush, K. 1996. Dust control material performance on unsurfaced roadways and tank trails. U.S. Army Environmental Center report SFIM-AEC-ET-CR-96196, 32 p.
- GBFIG (Galveston Bay Freshwater Inflows Group). 2003. Galveston Bay Freshwater Inflows. Houston Advanced Research Center, URL: http://trendstat.harc.edu/projects/fw_inflows/Gbfig.html (last accessed 6 January 2005).
- Giardino JR, Lynch K, Jennings D. 1995 Coupling rising sea level with process rates of geomorphic change: the Galveston Island paradigm. In Norwine J, Giardino JR, North GR, Valdes J. eds. *The Changing Climate of Texas*. Geobooks, College Station TX: 300-321
- GLO (Texas General Land Office). 2002. Shoreline Erosion Rates. <http://www.glo.state.tx.us/coastal/erosion/erosionrates.html>, accessed 12/17/02.
- Hall, S.L., Wilder, W. R., Fisher, F.M. 1986. An analysis of shoreline erosion along the northern coast of east Galveston Bay, Texas USA. *Journal of Coastal Research* 2: 173-179.
- Leatherman, S.P. 1984. Coastal geomorphic responses to sea level rise: Galveston Bay, Texas. In Barth, M.C., Titus, J.G., eds., *Greenhouse Effect and Sea Level Rise: A Challenge for this Generation*. New York: Van Nostrand Reinhold, pp. 5.1 - 5.24.
- Lester, J., Gonzalez, L. (eds). 2002. *The State of the Bay. A Characterization of the Galveston Bay Ecosystem* (2nd ed). Houston: Galveston Bay Estuary Program.
- McEwen, M.C. 1963. *Sedimentary Facies of the Trinity River Delta, Texas*. PhD dissertation, Rice University, Houston, 99 p
- Meade, R.H., 1982. Sources, sinks, and storage of river sediment in the Atlantic drainage of the United States. *Journal of Geology* 90, 235-252.
- Morton, R.A., 1977. Historical shoreline changes and their causes. *Transactions, Gulf Coast Association of Geological Societies* 27, 353-363
- Morton, R. A., 1993. *Shoreline Movement Along Developed Beaches of the Texas Gulf Coast: A Users' Guide to Analyzing and Predicting Shoreline Changes*. University of Texas at Austin, Bureau of Economic Geology Open-File Report 93-1, 79 pp.

- Morton, R.A., and Paine, J.G., 1990. Coastal land loss in Texas--an overview: Transactions, Gulf Coast Association of Geological Societies 40, 625-634.
- Nichols, M.M. 1989. Sediment accumulation rates and relative sea-level rise in lagoons. *Marine Geology* 88: 201-219.
- Phillips, J.D., Slattery, M.C., Musselman, Z.A. 2005. Channel adjustments of the lower Trinity River, Texas, downstream of Livingston Dam. *Earth Surface Processes and Landforms* (accepted for publication).
- Phillips, J.D., Slattery, M.C., Musselman, Z.A. 2004. Dam-to-delta sediment inputs and storage in the lower Trinity River, Texas. *Geomorphology* 62: 17-34.
- Phillips, J.D., 1991. Fluvial sediment delivery to a Coastal Plain estuary in the Atlantic Drainage of the United States. *Marine Geology* 98, 121-134.
- Phillips, J.D., 1992a. The source of alluvium in large rivers of the lower Coastal Plain of North Carolina. *Catena* 19, 59-75
- Phillips, J.D., 1992b. Delivery of upper-basin sediment to the lower Neuse River, North Carolina. *Earth Surface processes and Landforms* 17, 699-709
- Phillips, J.D., 1993. Pre- and post-colonial sediment sources and storage in the lower Neuse River basin, North Carolina. *Physical Geography* 14, 272-284.
- Phillips, J.D., 1995. Decoupling of sediment sources in large river basins In *Effects of Scale on Interpretation and Management of Sediment and Water Quality*. International Association of Hydrological Sciences pub. 226: 11-16
- Phillips, J.D., 2001. Sedimentation in bottomland hardwoods downstream of an east Texas dam. *Environmental Geology* 40, 860-868.
- Phillips, J.D. 2003. Toledo Bend Reservoir and geomorphic response in the lower Sabine River. *River Research and Applications* 19, 137-159.
- Phillips, J.D., Marion, D.F., 2001. Residence times of alluvium in an east Texas stream as indicated by sediment color. *Catena* 45, 49-71.
- Phillips, J.D., Musselman, Z.A., 2003. The effect of dams on fluvial sediment delivery to the Texas coast. *Proceedings of Coastal Sediments 2003*, American Society of Civil Engineers, 1-14.
- Rodriguez, A.B., Anderson, J.B., 2000. Mapping bay-head deltas within incised valleys as an aid for predicting the occurrence of barrier shoreline sands: an example from the Trinity/Sabine incised valley. *Gulf Coast Association of Geological Societies Transactions* 50, 755-758.
- Rodriguez, A., Anderson, J.B., and Bradford, J. "Holocene deltas of the Trinity Valley: analogs for exploration and production." *Gulf Coast Association of Geological Societies Transactions*, XLVIII (1998): 373-380.
- Rodriguez, A.B., Fassell, M.L., Anderson, J.B., 2001. Variations in shoreface progradation and ravinement along the Texas coast, Gulf of Mexico. *Sedimentology* 48, 837-853.
- Shepard, F.P. 1953. Sedimentation rates in Texas estuaries and lagoons. *Bulletin of the American Association of Petroleum Geologists* 37: 1919-1934.
- Smith, S.V., Renwick, W.H., Bartley, J.D., Buddemeier, R.W., 2002. Distribution and significance of small, artificial water bodies across the United States landscape. *Science of the Total Environment* 299, 2-36.
- Solis, R.S., Longley, W.L., Malstaff, G. 1994. Influence of inflow on sediment deposition in delta and bay systems. In: Longley, W.L., ed. *Freshwater Inflows to Texas Bays and Estuaries*. Texas Water Development Board, 56-70.
- Stork, S.V., Sneed, M. 2002. Houston-Galveston area from space--A new tool for mapping land subsidence. *U.S.*

Geological Survey Fact Sheet 110-002, URL: <http://water.usgs.gov/pubs/fs/fs-110-02/>

Sullivan, S., Thomas, D. Segura, S., Hulton, S., Elliott, W., Robichaud, M. 2003. Volumetric Survey of Lake Conroe. Austin: Texas Water Development Board, 33 p.

Thomas, M.A., Anderson, J.B., 1994. Sea-level controls on the facies architecture of the Trinity/Sabine incised-valley system, Texas continental shelf. In R.W. Dalrymple, R. Boyd, B.Z. Zaitline, eds., *Incised-Valley Systems: Origin and Sedimentary Sequences*. SEPM (Society for Sedimentary Geology), 63-82.

Van Metre, P.C., Sneek-Fahrer, D.A. 2002. Water Quality Trends in Suburban Houston, Texas, 1954-1997, as Indicated by Sediment Cores from Lake Houston. U.S. Geological Survey Fact Sheet 040-02, 6 p.

Welborn, C.T. 1967. Comparative results of sediment sampling with the Texas sampler and the depth-integrating samplers and specific weight of fluvial sediment deposits in Texas. Texas Water Development Board, 36 pp.

Wellmeyer, J.L., Slattery, M.C. and Phillips, J.D. 2005. Quantifying Downstream Impacts of Impoundment on Flow Regime and Channel Activity, Lower Trinity River, Texas. *Geomorphology* (accepted for publication).

White, W.A., Calnan, T.C., 1991. Submergence of vegetated wetlands in fluvial-deltaic area, Texas Gulf coast. In: *Coastal Depositional Systems of the Gulf of Mexico*. 12th Annual Research Conference, Society of Economic Paleontologists and Mineralogists, Gulf Coast Section, 278-279.

White, W.A., Morton, R.A., Holmes, C.W. 2002. A comparison of factors controlling sedimentation rates and wetland loss in fluvial-deltaic systems, Texas Gulf coast. *Geomorphology* 44, 47-66.

Appendix 1

Complete data set for the 138 potential source samples from the Trinity River system. All units as in Table 2.

Trinity River System - source samples

Field Label	JW label	Group	Lat	Long	(10-8) Xlf	Xarm	SIRM	X/Xarm	SIRM/X	Soft IRM	Hard IRM	-40 mT	-100 mT	-300 mT
TRD1	jwt	1	29.9097	94.7479	7.30	8.73	40.23	0.84	4.61	16.19	3.50	0.20	-0.43	-0.83
TRD2	jwt	2	29.9097	94.7479	4.55	1.92	40.84	2.37	21.27	16.90	4.36	0.17	-0.46	-0.79
TRD3	jwt	3	29.9155	94.7535	0.60	5.54	15.14	0.11	2.73	5.61	2.78	0.26	-0.47	-0.63
TRD4	jwt	4	29.9155	94.7535	1.50	5.24	25.80	0.29	4.92	15.52	2.32	-0.20	-0.66	-0.82
TRD5	jwt	5	29.9155	94.7535	6.40	4.32	46.09	1.48	10.66	19.37	5.45	0.16	-0.42	-0.76
TRD6	jwt	6	29.9117	94.7629	5.01	0.88	34.31	5.72	39.13	16.67	3.05	0.03	-0.56	-0.82
TRD7	jwt	7	29.9117	94.7629	6.40	3.86	47.93	1.66	12.41	19.42	5.03	0.19	-0.45	-0.79
TRD8	jwt	8	29.9091	94.7489	6.54	1.36	47.54	4.82	35.03	21.45	4.52	0.10	-0.51	-0.81
TRD9	jwt	9	29.9091	94.7489	5.50	3.93	46.82	1.40	11.90	19.57	4.00	0.16	-0.54	-0.83
TRD10	jwt	10	29.9091	94.7489	8.50	3.01	50.51	2.82	16.77	21.99	4.13	0.13	-0.55	-0.84
TRD11	jwt	11	29.8846	94.7393	7.09	2.34	61.04	3.03	26.06	22.76	5.84	0.25	-0.51	-0.81
TRD12	jwt	12	29.8846	94.7393	7.00	2.08	39.41	3.37	18.96	22.27	3.39	-0.13	-0.59	-0.83
TRD13	jwt	13	29.8846	94.7393	7.70	4.11	63.79	1.87	15.53	28.48	5.74	0.11	-0.54	-0.82
TRD14	jwt	14	29.8040	94.7432	4.80	4.08	32.78	1.18	8.03	14.63	3.58	0.11	-0.49	-0.78
TRD15	jwt	15	29.8120	94.7800	6.90	5.91	48.66	1.17	8.23	21.32	4.32	0.12	-0.54	-0.82
TRD16	jwt	16	29.8120	94.7800	3.30	1.66	25.06	1.98	15.06	13.00	2.25	-0.04	-0.64	-0.82
TRD17	jwt	17	29.8120	94.7800	1.40	1.51	31.17	0.93	20.61	20.03	1.00	-0.28	-0.83	-0.94
TRD18	jwt	18			5.90	3.79	38.20	1.56	10.07	17.02	3.57	0.11	-0.51	-0.81
TRD19	jwt	19			8.47	2.33	46.45	3.63	19.92	22.59	3.36	0.03	-0.57	-0.86
TRD20	jwt	20			5.60	6.10	43.77	0.92	7.17	18.21	3.83	0.17	-0.57	-0.82
TRD21	jwt	21			5.70	3.02	37.37	1.89	12.37	17.70	2.70	0.05	-0.59	-0.86
TRD22	jwt	22			9.06	2.14	64.28	4.22	29.97	25.83	5.23	0.20	-0.57	-0.84
TRD23	jwt	23			6.60	3.43	47.67	1.92	13.90	17.15	4.92	0.28	-0.44	-0.79
TRD24	jwt	24			8.18	2.11	56.19	3.88	26.66	24.74	5.09	0.12	-0.52	-0.82
TRD25	jwt	25			13.30	4.90	113.09	2.72	23.10	47.80	4.60	0.15	-0.64	-0.92
TRD26a	jwt	26			7.50	5.17	66.40	1.45	12.84	28.55	5.31	0.14	-0.57	-0.84
TRD26b	jwt	27			8.30	8.21	60.24	1.01	7.34	25.97	5.96	0.14	-0.60	-0.80
TRD27	jwt	28			6.60	4.37	68.07	1.51	15.59	35.62	6.41	-0.05	-0.61	-0.81
TRD28	jwt	29			6.70	3.26	68.65	2.06	21.06	29.84	14.10	0.13	-0.39	-0.59
TRD29	jwt	30			5.80	2.38	22.58	2.44	9.50	9.17	2.15	0.19	-0.45	-0.81
TRD30	jwt	31			8.40	4.08	65.98	2.06	16.18	31.64	6.16	0.04	-0.53	-0.81
TRD31	jwt	32			8.10	4.81	63.19	1.68	13.13	28.41	5.91	0.10	-0.53	-0.81
TRD32	jwt	33			9.60	3.13	40.78	3.07	13.04	16.27	5.22	0.20	-0.43	-0.74
TRD33	jwt	34			7.70	3.59	59.07	2.14	16.45	31.54	5.36	-0.07	-0.55	-0.82
TRD34	jwt	35			11.60	5.11	125.33	2.27	24.52	90.66	7.93	-0.45	-0.79	-0.87
TRD40	jwt	36			5.40	2.72	47.78	1.99	17.57	22.82	7.15	0.04	-0.48	-0.70
BT1	jwt	37	30.5821	94.6933	22.20	6.48	457.23	3.43	70.57	322.89	72.48	-0.41	-0.66	-0.68
BT2	jwt	38	30.5984	94.7076	60.70	31.94	1622.35	1.90	50.79	1083.56	319.61	-0.34	-0.57	-0.61
BT3	jwt	39	30.6111	94.7165	16.50	1.96	1098.00	8.41	559.51	6.93	965.30	0.99	0.96	0.76
BT4	jwt	40	30.6335	94.7165	7.40	5.94	80.78	1.25	13.61	45.06	11.17	-0.12	-0.50	-0.72
BT5	jwt	41	30.6335	94.7165	25.53	16.38	176.35	1.56	10.77	102.35	15.77	-0.16	-0.61	-0.82
BT6	jwt	42	30.6335	94.7165	10.20	3.69	92.28	2.77	25.02	58.90	12.20	-0.28	-0.59	-0.74
SHNF1	jwt	43	30.5607	95.1375	4.79	2.68	131.49	1.79	49.04	59.31	8.96	0.10	-0.53	-0.86
SHNF2	jwt	44	30.5154	95.1372	72.13	29.79	1698.21	2.42	57.00	1200.83	325.25	-0.41	-0.58	-0.62
SHNF3	jwt	45	30.5097	95.1138	9.10	2.45	528.03	3.72	215.65	21.79	450.27	0.92	0.86	0.71
SHNF4	jwt	46	30.5016	95.1028	61.20	31.68	2056.71	1.93	64.91	866.81	916.28	0.16	0.13	-0.11
SHNF5	jwt	47	30.5016	95.1028	15.40	7.33	306.56	2.10	41.81	221.25	27.77	-0.44	-0.70	-0.82
SHNF6	jwt	48	30.5150	95.0750	33.10	23.07	968.91	1.43	42.00	771.35	80.61	-0.59	-0.79	-0.83

SHNF7	jwt	49	3	30.5192	95.0693	101.60	168.89	2415.40	0.60	14.30	1967.07	155.62	-0.63	-0.82	-0.87
PCU1	jwt	50	4	30.7469	94.9562	11.00	3.56	61.98	3.09	17.41	26.54	11.15	0.14	-0.37	-0.64
PCU2	jwt	51	4	30.7606	94.9624	37.80	7.70	366.02	4.91	47.53	203.54	44.94	-0.11	-0.51	-0.75
PCU3	jwt	52	4	30.7606	94.9624	18.20	7.93	229.65	2.29	28.96	101.43	24.95	0.12	-0.46	-0.78
PCU4	jwt	53	4	30.7606	94.9624	12.70	7.41	218.54	1.71	29.49	98.33	24.81	0.10	-0.46	-0.77
PCU5	jwt	54	4	30.7687	94.9699	22.30	4.62	135.14	4.82	29.23	73.44	13.42	-0.09	-0.56	-0.80
PCU6	jwt	55	4	30.7687	94.9699	30.64	3.31	207.69	9.26	62.79	118.20	19.50	-0.14	-0.57	-0.81
PCU7	jwt	56	4	30.8066	94.9738	9.60	3.02	56.31	3.18	18.64	24.18	7.62	0.14	-0.49	-0.73
PCU8	jwt	57	4	30.8066	94.9738	9.10	3.64	115.94	2.50	31.85	53.63	30.35	0.07	-0.31	-0.48
PCU9	jwt	58	4	30.8083	94.9766	7.70	2.47	44.98	3.12	18.22	25.01	7.32	-0.11	-0.47	-0.67
PCU10	jwt	59	4	30.8083	94.9766	9.09	2.87	74.38	3.17	25.94	34.09	12.18	0.08	-0.43	-0.67
PCU11	jwt	60	4	30.8338	94.9777	10.50	3.88	103.81	2.70	26.73	37.82	32.75	0.27	-0.15	-0.37
PCU12	jwt	61	4	30.8855	94.8599	12.80	3.82	169.21	3.35	44.24	101.44	16.99	-0.20	-0.70	-0.80
PCU13	jwt	62	4	30.8934	94.8987	16.20	4.61	147.03	3.51	31.90	85.12	19.16	-0.16	-0.57	-0.74
PCU14	jwt	63	4	30.8416	94.9880	9.60	2.50	56.34	3.84	22.54	22.99	19.06	0.18	-0.16	-0.32
PCU15	jwt	64	4	30.8017	94.9915	4.82	2.75	67.48	1.75	24.53	32.29	6.58	0.04	-0.50	-0.81
LKC 1988 channel	jwt	65	5			0.00	1.34	9.62	0.00	7.17	2.51	3.14	0.48	0.00	-0.35
LKC headwaters	jwt	66	5	30.8835	94.8654	39.30	2.34	118.38	16.77	50.50	76.74	4.57	-0.30	-0.76	-0.92
LKC 942	jwt	67	5			1.48	1.51	17.09	0.98	11.36	8.83	1.31	-0.03	-0.61	-0.85
LKC channel hard layer	jwt	68	5			9.30	1.98	129.31	4.70	65.37	10.55	37.56	0.84	0.66	-0.42
Little CK SHNF	jwt	69	5			1.20	1.75	23.73	0.68	13.53	10.82	2.96	0.09	-0.41	-0.75
LMP gully floor	jwt	70	6			1.90	1.97	29.58	0.96	14.99	17.48	3.69	-0.18	-0.60	-0.75
LMP gully wall	jwt	71	6			9.90	3.50	103.00	2.83	29.40	49.24	14.37	0.04	-0.46	-0.72
LMP gully subsurface	jwt	72	6			16.40	5.29	186.23	3.10	35.21	120.35	9.97	-0.29	-0.81	-0.89
LMP upland	jwt	73	6			210.20	87.13	6986.19	2.41	80.18	5058.90	0.39	-0.45	-0.89	-1.00
Trinity @ Crockett flood deposit	jwt	74	7			9.70	6.59	69.03	1.47	10.48	31.96	9.82	0.07	-0.46	-0.72
Trinity River left bank bar downstream of 787 Romayor	jwt	75	7			0.60	1.22	17.31	0.49	14.24	9.39	2.25	-0.09	-0.56	-0.74
Trinity @ Romayor cut bank	jwt	76	7			6.17	1.78	42.23	3.48	23.79	11.88	12.26	0.44	0.06	-0.42
Trinity river channel @ Liberty	jwt	77	7			1.90	1.95	20.78	0.98	10.66	9.21	2.20	0.11	-0.45	-0.79
Trinity @ Liberty floodplain	jwt	78	7			8.60	3.81	57.33	2.26	15.04	24.21	5.91	0.16	-0.50	-0.79
Trinity River @ 105 sandbar	jwt	79	7			10.50	5.27	113.56	1.99	21.56	90.10	3.57	-0.59	-0.88	-0.94
Trinity @ Crockett channel margin	jwt	80	7			6.73	2.62	54.71	2.57	20.91	24.08	6.87	0.12	-0.46	-0.75
Trinity @ 105 floodplain	jwt	81	7			8.10	3.80	64.95	2.13	17.11	28.08	5.48	0.14	-0.53	-0.83
Trinity @ mouth of Long King	jwt	82	7			7.80	2.51	41.85	3.11	16.70	25.22	2.83	-0.21	-0.65	-0.86
Trinity @ 3278 channel bed	jwt	83	7			5.20	2.22	39.55	2.34	17.78	22.51	6.64	-0.14	-0.48	-0.66
Trinity @ 3278 channel	jwt	84	7			9.22	1.86	55.95	4.96	30.11	25.24	9.94	0.10	-0.40	-0.64
Trinity Delta @ Ft Ananuac	jwt	85	7			5.00	3.85	42.72	1.30	11.09	18.12	4.30	0.15	-0.49	-0.80
Trinity River @ 105 channel	jwt	86	7			0.50	1.21	9.32	0.41	7.73	3.83	1.49	0.18	-0.42	-0.68
Trinity @ 3278 bank scarp	jwt	87	7			9.10	3.59	69.42	2.54	19.35	25.73	13.56	0.26	-0.29	-0.61
Trinity @ Liberty sandbar	jwt	88	7			0.20	1.28	8.17	0.16	6.38	3.22	1.27	0.21	-0.39	-0.69
Trinity @ Bank 3728	jwt	89	7			9.07	1.57	38.76	5.76	24.63	12.19	8.84	0.37	-0.20	-0.54
Trinity @ Romayor cutbank	jwt	90	7			1.50	2.20	19.22	0.68	8.73	6.83	6.23	0.29	-0.18	-0.35
Menard CK 146 Tr. Youtory	jwt	91	8			3.50	2.35	49.75	1.49	21.21	32.32	5.85	-0.30	-0.66	-0.76
Menard CK 943	jwt	92	8			10.40	3.65	56.34	2.85	15.42	23.25	5.86	0.17	-0.46	-0.79
Menard CK mouth	jwt	93	8			5.57	2.19	47.68	2.54	21.76	21.47	4.57	0.10	-0.51	-0.81
Menard CK Soda East Loop	jwt	94	8			10.70	3.65	58.34	2.93	15.98	35.11	10.09	-0.20	-0.53	-0.65
Big CK 150	jwt	95	9			-0.10	1.37	7.19	-0.07	5.25	2.88	1.06	0.20	-0.41	-0.71
Big CK BCSA channel	jwt	96	9			15.50	15.89	348.18	0.98	21.92	228.31	71.43	-0.31	-0.54	-0.59
Big CK 222 channel	jwt	97	9			0.74	1.19	9.86	0.62	8.32	4.78	1.03	0.03	-0.56	-0.79
Dayton Lakes cutbank	jwt	98	10			9.50	3.43	58.75	2.77	17.12	23.91	8.02	0.19	-0.43	-0.73
Dayton Lakes channel	jwt	99	10			9.50	3.39	52.04	2.81	15.37	25.06	4.88	0.04	-0.53	-0.81
Pecan Landing flood deposit	jwt	100	10			11.90	8.23	89.84	1.45	10.91	40.90	12.51	0.09	-0.48	-0.72
Pecan Landing point bar	jwt	101	10			0.40	1.45	11.25	0.28	7.77	4.52	2.22	0.20	-0.32	-0.61
Pecan Landing channel margin	jwt	102	10			1.50	1.68	13.55	0.89	8.06	5.84	2.89	0.14	-0.35	-0.57

Moss Hill Tree 3	jwt	103	10	10.40	3.98	105.48	2.62	26.53	62.96	5.14	-0.19	-0.70	-0.90	
Moss Hill Tree 5	jwt	104	10	8.20	3.38	55.77	2.42	16.48	23.97	4.62	0.14	-0.54	-0.83	
Long King @ 190 sand	jwt	105	10	2.92	1.86	25.78	1.57	13.87	14.61	2.88	-0.13	-0.63	-0.78	
Long King @ 190 mud	jwt	106	10	10.90	2.36	70.39	4.62	29.82	30.09	18.53	0.15	-0.24	-0.47	
SHLE channel (Trinity)	jwt	107	10	6.41	1.76	32.02	3.65	18.20	17.12	3.73	-0.07	-0.52	-0.77	
SHLE cutbank	jwt	108	10	7.10	2.64	44.31	2.69	16.81	19.12	5.14	0.14	-0.39	-0.77	
Romayor Bedrock	jwt	109	10	16.10	3.15	105.39	5.11	33.44	41.42	37.95	0.21	-0.10	-0.28	
Kenefick cutbank	jwt	110	10	19.78	2.16	78.42	9.14	36.24	48.29	7.78	-0.23	-0.59	-0.80	
Kenefick channel	jwt	111	10	0.30	1.18	8.92	0.26	7.59	3.06	1.83	0.31	-0.33	-0.59	
Long Tom CK 942	jwt	112	10	3.73	1.61	28.91	2.32	17.95	15.60	2.29	-0.08	-0.60	-0.84	
Burnett CK 942	jwt	113	10	0.80	1.33	11.98	0.60	9.00	5.23	1.97	0.13	-0.48	-0.67	
Tempe CK	jwt	114	10	7.40	2.63	33.18	2.82	12.63	19.26	1.79	-0.16	-0.70	-0.89	
Huffman CK 222 channel	jwt	115	10	0.40	1.62	21.20	0.25	13.06	14.25	2.28	-0.34	-0.64	-0.78	
Cypress Lakes beach channel	jwt	116	10	0.70	1.16	8.30	0.60	7.14	3.20	2.08	0.23	-0.24	-0.50	
Goodrich FP Tree 1	jwt	117	10	11.80	3.06	55.77	3.86	18.23	32.33	4.80	-0.16	-0.60	-0.83	
Bedias CK mouth channel	jwt	118	10	11.80	9.35	87.41	1.26	9.35	42.52	13.62	0.03	-0.45	-0.69	
1 (samples collected with Mike 05-04)	jwt	119	11	7.00	3.27	49.15	2.14	15.03	21.16	4.61	0.14	-0.50	-0.81	
2	jwt	120	11	8.60	3.11	44.73	2.77	14.38	17.24	5.17	0.23	-0.35	-0.77	
3	jwt	121	11	8.70	3.57	49.73	2.44	13.92	24.52	4.81	0.01	-0.54	-0.81	
4	jwt	122	11	4.60	3.51	52.22	1.31	14.88	29.22	4.11	-0.12	-0.59	-0.84	
5	jwt	123	11	14.30	4.62	140.37	3.09	30.37	88.19	8.77	-0.26	-0.75	-0.88	
6	jwt	124	11	10.40	2.34	40.97	4.45	17.51	23.12	2.60	-0.13	-0.63	-0.87	
7	jwt	125	11	4.80	3.48	83.97	1.38	24.14	33.59	8.36	0.20	-0.40	-0.80	
8	jwt	126	11	6.60	5.43	121.13	1.22	22.32	51.35	14.49	0.15	-0.38	-0.76	
9	jwt	127	11	7.50	4.39	78.30	1.71	17.85	35.20	9.30	0.10	-0.42	-0.76	
10	jwt	128	11	23.70	13.25	115.74	1.79	8.73	71.02	20.32	-0.23	-0.39	-0.65	
11	jwt	129	11	6.00	2.97	39.04	2.02	13.16	21.31	3.08	-0.09	-0.60	-0.84	
12	jwt	130	11	11.60	2.94	47.53	3.95	16.18	28.72	3.14	-0.21	-0.68	-0.87	
13	jwt	131	11	11.20	4.57	100.95	2.45	22.09	45.16	6.36	0.11	-0.50	-0.87	
14	jwt	132	11	7.60	4.67	68.26	1.63	14.63	30.83	6.88	0.10	-0.51	-0.80	
15	jwt	133	11	7.00	4.23	64.78	1.66	15.32	29.64	5.67	0.08	-0.54	-0.82	
16	jwt	134	11	8.90	3.46	52.03	2.57	15.05	27.77	4.57	-0.07	-0.56	-0.82	
17	jwt	135	11	7.00	7.54	117.21	0.93	15.53	61.38	8.72	-0.05	-0.57	-0.85	
18	jwt	136	11	5.00	3.77	62.27	1.33	16.53	32.70	4.72	-0.05	-0.58	-0.85	
19	jwt	137	11	11.30	7.36	119.69	1.53	16.25	69.35	14.28	-0.16	-0.56	-0.76	
20	jwt	138	11	5.00	2.86	36.57	1.75	12.77	16.94	3.62	0.07	-0.54	-0.80	
				Mean	12.07	6.29	195.27	2.45	26.33	115.58	31.84	0.03	-0.48	-0.73
				St Dev	21.49	16.39	677.44	2.00	50.57	483.56	123.79	0.25	0.25	0.23
				Min	-0.10	0.88	7.19	-0.07	2.73	2.51	0.39	-0.63	-0.89	-1.00
				Lower Quartile	5.25	2.21	39.72	1.38	12.89	17.18	3.57	-0.13	-0.59	-0.82
				Median	7.75	3.41	56.32	2.12	16.79	25.04	5.57	0.09	-0.52	-0.79
				Upper Quartile	10.65	4.62	103.61	3.06	25.71	44.43	11.93	0.16	-0.43	-0.69
				Max	210.20	168.89	6986.19	16.77	559.51	5058.90	965.30	0.99	0.96	0.76
TRD samples				17	6.40	3.86	40.84	1.66	15.06	19.42	4.00	0.12	-0.54	-0.82
BT				6	19.35	6.21	316.79	2.33	37.91	80.62	44.13	-0.22	-0.58	-0.70
SHNF				7	33.10	23.07	968.91	1.93	49.04	771.35	155.62	-0.41	-0.58	-0.82
PCU				15	11.00	3.64	115.94	3.17	28.96	53.63	19.06	0.07	-0.47	-0.74

Appendix 2: Sediment rating curves for Romayor and it's tributaries.

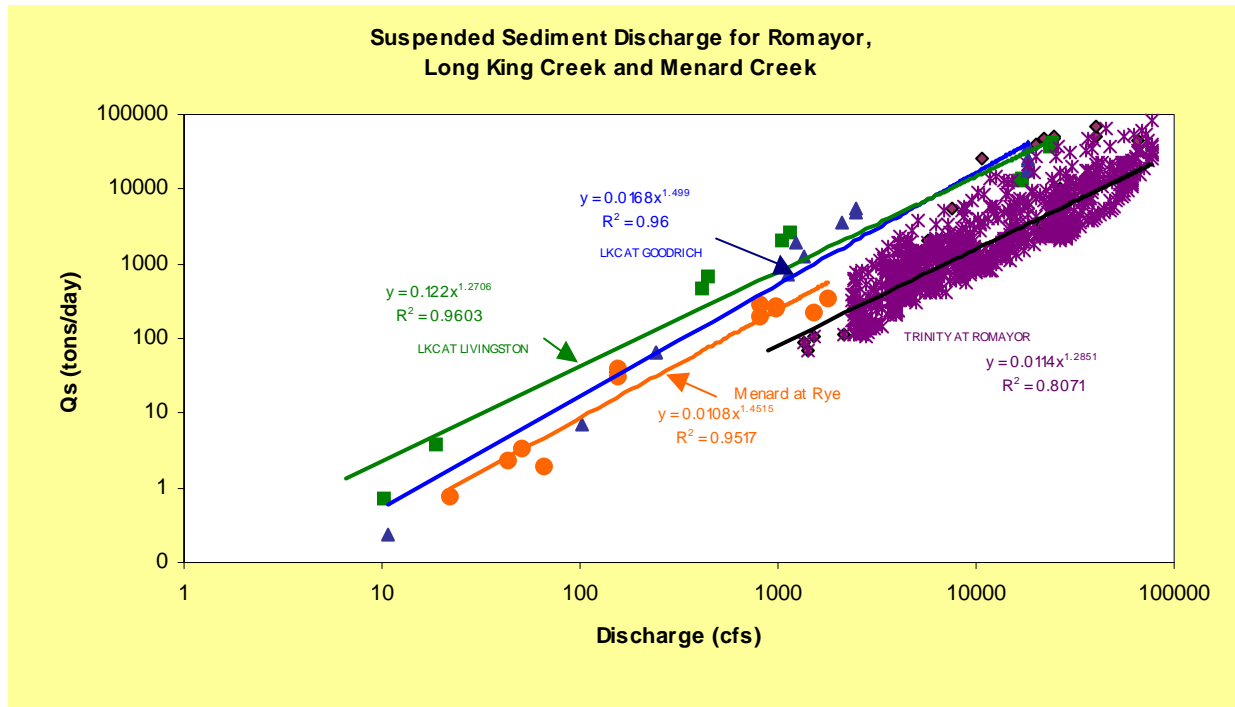


Fig 1. Sediment rating curves for Romayor, Long King Creek at both Livingston and Goodrich, and Menard Creek. Note that for Romayor, the depth-integrated (diamonds) and turbidity-generated (purple x's) are shown.

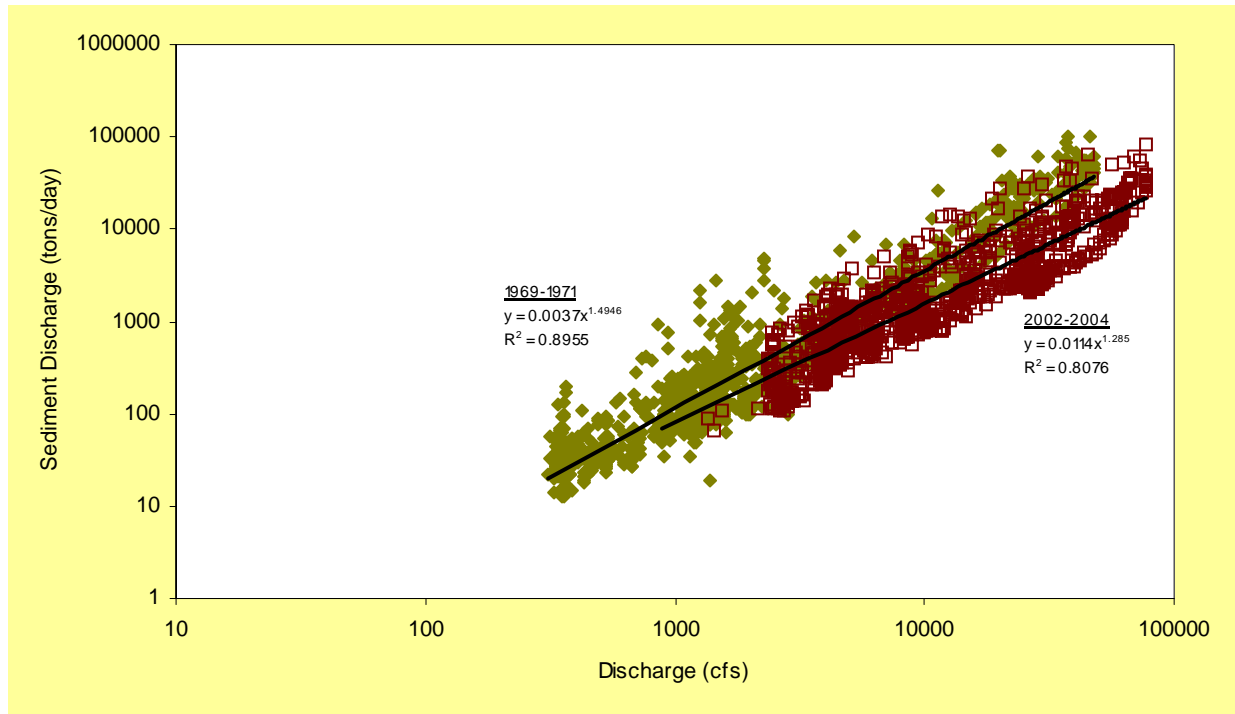


Fig 2. Sediment rating curves for Romayor for 1969-1971 (TWDB data post-dam) and turbidity-generated data for 2002-2004.

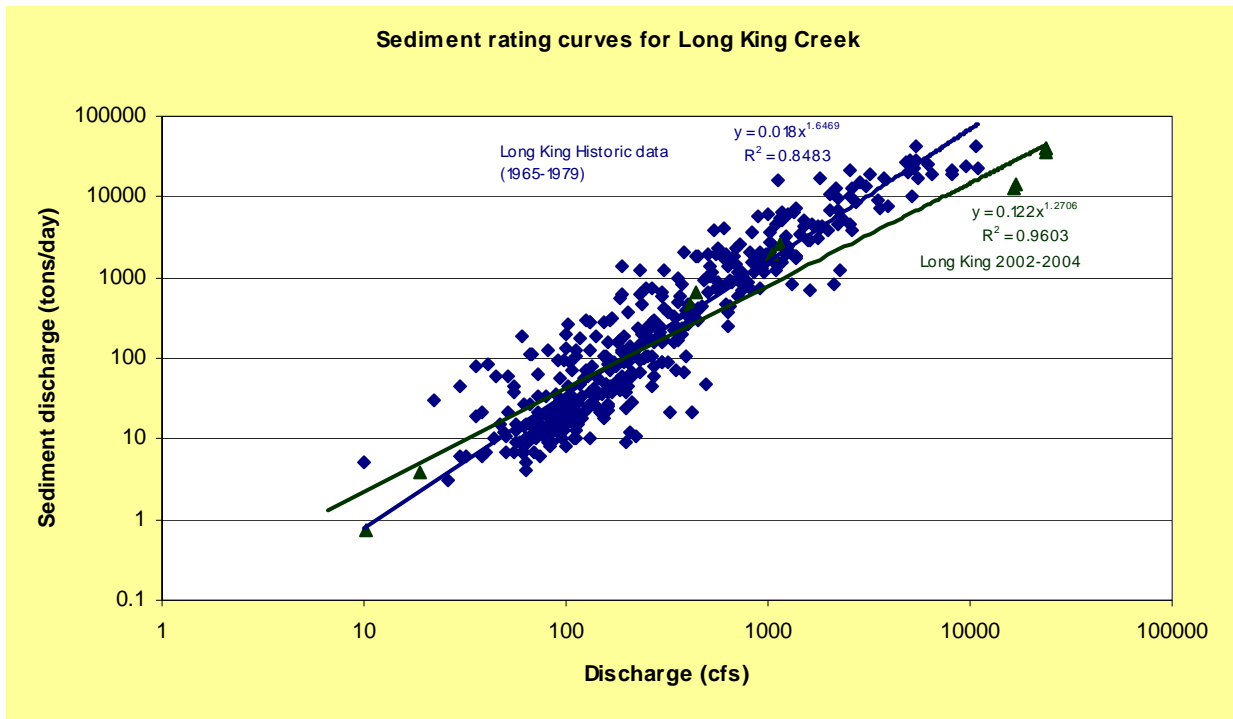


Fig 3. Sediment rating curves for Long King Creek at Livingston for selected events during the period 1965-1979 (TWDB data) and depth-integrated data for 2002-2004.

